

**CROSS-LAYER DESIGN FOR WIRELESS AD HOC SENSOR
NETWORKS**

by
XINSHENG XIA

A Ph.D Dissertation Proposal
Presented to the Faculty of the Graduate School of
The University of Texas at Arlington in Partial Fulfillment
of the Requirements
for the Degree of

DOCTOR OF PHILOSOPHY

THE UNIVERSITY OF TEXAS AT ARLINGTON

December 2007

Copyright © by Xincheng Xia 2007

All Rights Reserved

ACKNOWLEDGEMENTS

Though the following dissertation is an individual work, I could never have reached the heights or explored the depths without the help, support, guidance and efforts of a lot of people.

My deepest gratitude is to my advisor, Dr. Qilian Liang. I have been amazingly fortunate to have an advisor who gave me the freedom to explore on my own, and at the same time the guidance to recover when my steps faltered. Dr. Liang taught me how to question thoughts and express ideas. His patience and support helped me overcome many crisis situations and finish this dissertation. Dr. Liang, has been always there to listen and give advice. I am deeply grateful to him for the long discussions that helped me sort out the technical details of my work. I am also thankful to him for encouraging the use of correct grammar and consistent notation in my writings and for carefully reading and commenting on countless revisions of this manuscript. Dr. Liang's insightful comments and constructive criticisms at different stages of my research were thought-provoking and they helped me focus my ideas. I am grateful to him for holding me to a high research standard and enforcing strict validations for each research result, and helping me not only in research area.

I am grateful to Dr. Michael Manry, Dr. Soontorn Oraintara, Dr. Dan Popa, Dr. Saibun Tjuatja, and Dr. Zhou Wang for their encouragement and practical advice. I am also thankful to them for reading my dissertation, commenting on my views, and taking time to serve in my dissertation committee.

I am also grateful to the former or current faculty and staff at University of Texas at Arlington, for their various forms of support during my graduate study.

I would like to acknowledge my colleague in wireless communication and networking laboratory: Dr. Liang Zhao, Dr. Lingming Wang, Dr. Haining Shu, Jing Liang, Qingchun Ren and other friends for numerous discussions on related topics that helped me improve my knowledge in research area.

Many other friends have helped me stay sane through these difficult years. Their support and care helped me overcome setbacks and stay focused on my graduate study. I greatly value their friendship and I deeply appreciate their belief in me.

Most importantly, none of this would have been possible without the love and patience of my family. My family to whom this dissertation is dedicated to, has been a constant source of love, concern, support and strength all these years. I would like to express my heart-felt gratitude to my family.

November 27, 2007

ABSTRACT

CROSS-LAYER DESIGN FOR WIRELESS AD HOC SENSOR NETWORKS

Xinsheng Xia

The University of Texas at Arlington, 2007

Supervising Professor: Qilian Liang

Cross-layer design is an efficient approach to enhance energy efficiency and Quality of Service (QoS) in wireless ad hoc sensor networks. This dissertation will focus on the cross-layer issues and approaches. It will also discuss the latency-aware and energy efficiency tradeoffs and the packets transmission in the rear part of the dissertation.

Firstly, we will analyze the cross-layer design for wireless sensor networks based on the virtual MIMO techniques. We will coordinate the physical layer, the MAC layer and the network layer for cross-layer evaluation. Performance analysis and simulation results show that throughput and packet loss ratio will have different performances compared with only considering the MIMO scheme in the physical layer as the increase of the number of transmitters.

Secondly, we will discuss the bottom-up optimization for cross-layer design. We used the fuzzy logic system (FLS) to coordinate the physical layer, the data-link layer and the application layer for cross-layer design. Simulation results show that the cross-layer design can reduce the average delay, increase the throughput and extend the network lifetime. The network performance parameters could also keep stability after the cross-layer optimization.

Thirdly, we extended the FLS application in cross-layer design from Type-1 to Type-2. We demonstrated that type-2 fuzzy membership function (MF), i.e., the Gaussian MFs with uncertain variance is most appropriate to model BER and MAC layer service time. We used the forecasted transmission delay to adjust the transmission power, and it showed that the interval type-2 FLS performed much better than a type-1 FLS, and FLSs performed better than back-prop NN in terms of energy consumption, average delay and throughput. Also, we obtained the performance bound based on the actual transmission delay.

Finally, we applied a image as the real service in WSNs. We considered cross-layer design for image transmission in WSNs. We combined the application layer, the MAC layer and the physical layer together. According to analysis and simulation, there were tradeoffs between QoS and energy consumption for both high priority service and low priority service. Application level QoS was applied to evaluate the cross-layer design for WSNs.

Two other works were discussed in this dissertation. One is the latency-aware and energy efficiency tradeoffs for wireless sensor networks. The FLS is applied to the nodes selection. In contrast with the cases that only consider one descriptor, the FLS application can manage the delay/energy tradeoffs to meet the network performance requirements. Another work discussed is "Packets Transmission in wireless sensor networks: interference, energy and delay-aware approach". We proposed FLS in the optimization of SIR threshold selection. Average delay and distance of a node to the source node are selected as antecedents for the FLS. The output of FLS provided adjusting factors for the SIR threshold. Simulation results showed the fuzzy optimization could achieve a better network efficiency, reduce the average delay and extend the network lifetime.

TABLE OF CONTENTS

| | |
|--|-----|
| ACKNOWLEDGEMENTS | iii |
| ABSTRACT | v |
| LIST OF FIGURES | xii |
| LIST OF TABLES | xiv |
| Chapter | |
| 1. INTRODUCTION | 1 |
| 1.1 Wireless Sensor Networks | 1 |
| 1.2 Cross-layer Design | 2 |
| 1.2.1 Classification of Cross-layer Solution | 3 |
| 1.3 Research Motivation | 4 |
| 1.4 Classification of QoS Categories | 4 |
| 1.5 Contribution | 5 |
| 1.6 Preliminories | 6 |
| 1.6.1 Architecture of OSI Structure | 6 |
| 1.6.2 IEEE 802.11a OFDM PHY | 6 |
| 1.6.3 IEEE 802.11 MAC | 7 |
| 1.7 Network Layer | 8 |
| 1.7.1 Application Layer | 9 |
| 1.7.2 Energy | 11 |
| 1.7.3 Delay | 11 |
| 1.7.4 Node Mobility and Channel Fading | 12 |
| 1.7.5 One-step Markov Path Model | 14 |

| | | |
|-------|--|----|
| 1.8 | Dissertation Structure | 14 |
| 2. | CROSS-LAYER DESIGN FOR WSNS BASED ON MIMO TECHNIQUES . . | 16 |
| 2.1 | Introduction | 16 |
| 2.2 | Preliminaries | 17 |
| 2.2.1 | IEEE 802.11a OFDM PHY | 17 |
| 2.2.2 | IEEE 802.11 MAC | 17 |
| 2.2.3 | Network Layer | 18 |
| 2.2.4 | Node Mobility and Channel Fading | 18 |
| 2.3 | Performance Analysis | 20 |
| 2.3.1 | MIMO | 20 |
| 2.3.2 | IEEE 802.11 MAC Protocol | 22 |
| 2.3.3 | AODV Routing Protocol | 24 |
| 2.4 | Cross-layer Analysis | 25 |
| 2.4.1 | Throughput | 25 |
| 2.4.2 | Packet Loss Ratio | 26 |
| 2.5 | Simulations and Analysis | 26 |
| 2.5.1 | Throughput | 27 |
| 2.5.2 | Packet Loss Ratio | 28 |
| 2.6 | Conclusion and Analysis | 29 |
| 3. | BOTTOM-UP CROSS-LAYER OPTIMIZATION FOR MANET | 30 |
| 3.1 | Introduction | 30 |
| 3.2 | Overview of Fuzzy Logic Systems | 30 |
| 3.3 | Fuzzy Application For Cross-layer Design | 31 |
| 3.4 | Simulations | 34 |
| 3.4.1 | Average Delay | 35 |
| 3.4.2 | Energy Efficiency | 35 |

| | | |
|-------|--|----|
| 3.4.3 | Network Efficiency | 36 |
| 3.5 | Conclusions | 38 |
| 4. | CROSS-LAYER DESIGN FOR MOBILE AD HOC NETWORKS USING INTERVAL TYPE-2 FUZZY LOGIC SYSTEMS | 40 |
| 4.1 | Introduction | 40 |
| 4.2 | Preliminaries | 40 |
| 4.2.1 | Bit Error Rate | 40 |
| 4.2.2 | MAC Layer Service Time | 40 |
| 4.2.3 | Packet Transmission Delay | 41 |
| 4.3 | Overview of Interval Type-2 Fuzzy Logic Systems | 41 |
| 4.4 | Modeling BER and MAC Layer Service Time Using Interval Type-2 Membership Function | 44 |
| 4.4.1 | BER Analysis and Modeling BER | 44 |
| 4.4.2 | MAC Layer Service Time Analysis and Modeling | 46 |
| 4.5 | Cross-Layer Design Using Interval Type-2 Fuzzy Logic System | 47 |
| 4.6 | Simulations | 49 |
| 4.6.1 | Average Delay | 50 |
| 4.6.2 | Energy Efficiency | 52 |
| 4.6.3 | Networks Efficiency | 53 |
| 4.7 | Conclusion | 54 |
| 5. | CROSS-LAYER DESIGN FOR IMAGE TRANSMISSION IN WIRELESS SENSOR NETWORKS | 55 |
| 5.1 | Introduction | 55 |
| 5.2 | Overview of Cross-layer Design | 55 |
| 5.3 | Simulation and Analysis | 56 |
| 5.3.1 | Packet Successful Transmission Ratio | 57 |
| 5.3.2 | Average Delay | 58 |

| | | |
|-------|---|----|
| 5.3.3 | Energy Efficiency | 59 |
| 5.3.4 | Image Quality | 60 |
| 5.4 | Conclusion | 61 |
| 6. | LATENCY-AWARE AND ENERGY EFFICIENCY TRADEOFFS FOR WIRELESS SENSOR NETWORKS | 63 |
| 6.1 | Introduction | 63 |
| 6.2 | Energy And The 2-Hop Relay Algorithm | 65 |
| 6.2.1 | Energy | 65 |
| 6.2.2 | The Two-hop Relay Algorithm | 65 |
| 6.2.3 | Cell Location Algorithm | 66 |
| 6.2.4 | In-cell Feedback Algorithm | 67 |
| 6.3 | The FLS application for the two-hop relay algorithm | 67 |
| 6.4 | Simulation | 70 |
| 6.4.1 | Average Latency | 70 |
| 6.4.2 | Energy Efficiency | 71 |
| 6.4.3 | Network quality | 73 |
| 6.4.4 | FLS vs Mobility | 74 |
| 6.4.5 | FLS vs the Remaining Energy | 75 |
| 6.5 | Conclusion | 76 |
| 7. | PACKETS TRANSMISSION IN WIRELESS SENSOR NETWORKS: INTERFERENCE, ENERGY, AND DELAY-AWARE APPROACH | 80 |
| 7.1 | Introduction | 80 |
| 7.2 | Preliminaries | 82 |
| 7.2.1 | Co-channel Interference | 82 |
| 7.2.2 | Queueing Model | 82 |
| 7.2.3 | Delay | 83 |

| | | |
|----------|--------------------------------------|-----|
| 7.3 | Fuzzy Optimization | 83 |
| 7.4 | Simulations | 85 |
| 7.4.1 | Average Delay | 86 |
| 7.4.2 | Energy Efficiency | 86 |
| 7.4.3 | Network quality | 88 |
| 7.5 | Conclusion | 88 |
| 8. | CONCLUSION AND FUTURE WORK | 95 |
| 8.1 | Conclusions | 95 |
| 8.2 | Future Work | 96 |
| Appendix | | |
| A. | AVERAGE BER PERFORMANCE | 98 |
| B. | PUBLICATION LIST | 100 |
| | REFERENCES | 103 |
| | BIOGRAPHICAL STATEMENT | 110 |

LIST OF FIGURES

| Figure | Page |
|--|------|
| 1.1 OSI Stack | 7 |
| 1.2 General Behavior of a Congestion-controlled System | 10 |
| 1.3 BER Curves with Rayleigh Fading and Different Modulation | 13 |
| 1.4 One-step Markov Path Model | 14 |
| 2.1 Diversity-multiplexing trade-offs | 22 |
| 2.2 System Architecture for cross-layer design | 27 |
| 2.3 Throughput Vs Number of Transmitters | 28 |
| 2.4 PLR Vs Number of Transmitters | 29 |
| 3.1 The structure of a fuzzy logic system | 30 |
| 3.2 Cross-layer Design Algorithm | 32 |
| 3.3 MFs for antecedents | 33 |
| 3.4 MFs for consequents | 34 |
| 3.5 The Average Delay Versus Simulation Times | 36 |
| 3.6 Number of Nodes Alive Versus Simulation Time | 37 |
| 3.7 Throughput Versus Simulation Time | 38 |
| 4.1 The structure of a type-2 FLS | 42 |
| 4.2 Type-2 Gaussian MF with uncertain standard deviation | 46 |
| 4.3 FLS application for cross-layer design | 49 |
| 4.4 The RMSE of packet transmission delay prediction | 51 |
| 4.5 Average Delay for Three Algorithms | 51 |
| 4.6 Remaining Energy for Three Algorithms | 52 |

| | | |
|-----|---|----|
| 4.7 | Throughput for Three Algorithms | 53 |
| 5.1 | Structure of Cross-layer Design | 55 |
| 5.2 | Packet Successful Transmission Ratio | 58 |
| 5.3 | Average Delay | 59 |
| 5.4 | Remaining Energy | 60 |
| 5.5 | The Image Results | 62 |
| 6.1 | A Cell-partitioning Wireless Sensor Network | 63 |
| 6.2 | MFs for antecedents | 69 |
| 6.3 | MFs for consequent | 69 |
| 6.4 | Average latency performance of the two algorithms | 71 |
| 6.5 | Sensor nodes alive of the two algorithms | 73 |
| 6.6 | Remaining energy of the two algorithms | 74 |
| 6.7 | Packets received of the two algorithms | 75 |
| 6.8 | The FLS application vs the degree of mobility. | 76 |
| 6.9 | The FLS application vs the remaining energy. | 77 |
| 7.1 | TDMA frame | 91 |
| 7.2 | (a) MFs for Antecedents (b) MFs for Consequents | 91 |
| 7.3 | Control Surface | 92 |
| 7.4 | Average Delay (a) Constant Thresholds (b) Fuzzy Optimization | 92 |
| 7.5 | Energy Efficiency. (a) Constant Thresholds (b) Fuzzy Optimization | 93 |
| 7.6 | Packets Received.(a) Constant Thresholds (b) Fuzzy Optimization | 94 |

LIST OF TABLES

| Table | | Page |
|-------|--|------|
| 1.1 | Eight PHY Modes of the IEEE802.11A PHY | 8 |
| 3.1 | The fuzzy rules for cross-layer design | 39 |
| 4.1 | Mean and std values for BER. | 45 |
| 4.2 | Mean and std values for logarithm of MAC layer service time | 47 |
| 4.3 | Fuzzy Rules and Consequent | 48 |
| 5.1 | Design Cases | 57 |
| 5.2 | Parameters Setting | 57 |
| 5.3 | Image Quality | 61 |
| 6.1 | The questions for Nodes Election for the two-Hop Relay Algorithm | 78 |
| 6.2 | Histograms of expert responses. | 79 |
| 7.1 | Fuzzy Rules and Consequent | 90 |

CHAPTER 1

INTRODUCTION

1.1 Wireless Sensor Networks

Wireless sensor network (WSN) is a wireless network consisting of spatially distributed autonomous devices using sensors to cooperatively monitor physical or environmental conditions, such as temperature, sound, vibration, pressure, motion or pollutants, at different locations [5]. It can be thought as ad hoc network consisting of sensor nodes linked by a wireless medium to perform distributed sensing tasks. The development of wireless sensor networks was originally motivated by military applications such as battlefield surveillance. However, wireless sensor networks are now used in many civilian application areas, including environment and habitat monitoring, healthcare applications, home automation, and traffic control [2].

Although WSNs have unlimited potential, many research challenges exist [3] [4] [5]:

1. Power management: Low-cost deployment is one acclaimed advantage of sensor networks. However, the energy constraint is unlikely to be solved soon due to slow progress in developing battery capacity. Moreover, the untended nature of sensor nodes and hazardous sensing environments preclude battery replacement as a feasible solution. On the other hand, the surveillance nature of many sensor network applications requires a long lifetime; therefore, it is a very important research issue to provide a form of energy-efficient surveillance service for a geographic area.

2. Real-time: WSN deal with real world environments. In many cases, sensor data must be delivered within time constraints so that appropriate observations can be made or actions taken. Very few results exist to date regarding meeting real-time requirements

in WSN. Most protocols either ignore real-time or simply attempt to process as fast as possible and hope that this speed is sufficient to meet deadlines.

3. Security and Privacy: WSN are limited in their energy, computation, and communication capabilities. In contrast to traditional networks, sensor nodes are often deployed in accessible areas, presenting a risk of physical attacks. Sensor networks interact closely with their physical environment and with people, posing additional security problems. Because of these reasons current security mechanisms are inadequate for WSN. These new constraints pose new research challenges on key establishment, secrecy and authentication, privacy, robustness to denial-of-service attacks, secure routing, and node capture.

1.2 Cross-layer Design

The demand for energy efficiency and QoS in wireless ad hoc sensor networks is growing in a rapid speed. To enhance the energy efficiency and QoS, we consider the combination of physical layer, data-link layer and application layer together, a cross-layer approach. A strict layered design is not flexible enough to cope with the dynamics of the mobile ad hoc networks [6]. Cross-layer design could introduce the layer interdependencies to optimized overall network performance. The general methodology of cross-layer design is to maintain the layered architecture, capture the important information that influence other layers, exchange the information between layers and implement adaptive protocols and algorithms at each layer to optimize the performance.

Lots of previous works have focused on cross-layer design for QoS provision. Liu [7] combine the AMC at physical layer and ARQ at the data link layer. Ahn [8] use the info from MAC layer to do rate control at network layer for supporting real-time and best effort traffic. Akan [9] propose a new adaptive transport layer suite including adaptive

transport protocol and adaptive rate control protocol based on the lower layer information.

Some works related to energy efficiency have been reported. Banbos proposes a power-controlled multiple access schemes in [10]. This protocol reveals the trade-off of the transmitter power cost and backlog/delay cost in power control schemes. Zhu [11] proposes a minimum energy routing scheme, which consider the energy consumption for data packets as well as control packets of routing and multiple access. In [12], Sichitiu proposes a cross-layer scheduling method. Through combining network layer and MAC layer, a deterministic, schedule-based energy conservation scheme is proposed. This scheme drives its power efficiency from eliminating idle listening and collisions.

However, cross-layer design can produce unintended interactions among protocols, such as an adaptation loops. It is hard to characterize the interaction at different layers and joint optimization across layers may lead to complex algorithm.

1.2.1 Classification of Cross-layer Solution

Top-down approach [13]: the high-layer protocols optimize their parameters and strategies at the next lower layer. This cross-layer solution has been deployed in most exciting systems.

Bottom-up approach: the lower layers try to insulate the higher layers from the losses and bandwidth variations. This cross-layer solution is not optimal for multimedia transmission, duo to the incurred delay and unnecessary throughput reduction.

Application-centric approach: the application layer optimizes the lower layer parameters one at a time in a bottom-up or top-down manner.

MAC-centric approach: In this approach the APP layer passes its traffic information and requirements to the MAC, which decides which APP layer packets/flows should

be transmitted and at what QoS level. The MAC also decides the PHY layer parameters based on the available channel information.

Integrated approach: In this approach, strategies are determined jointly. Unfortunately, exhaustively trying all the possible strategies and their is impractical due to the associated complexity. A possible solution to solve this complex cross-layer optimization problem in an integrated manner is to use learning and classification techniques.

1.3 Research Motivation

Energy Efficiency: as a micro-electronic device, sensor node can be equipped with a limited power source. Besides, most of the wireless sensor networks are set remotely, it is impossible to replenish the power source.

QoS: QoS is defined as a set of requirements, such as delay, delay jitter, bandwidth, and packet successful transmission ratio, which must be met in transporting a packet in order to support application function.

1.4 Classification of QoS Categories

Bit-level QoS - to ensure the accuracy of transmission, a maximum BER for each wireless node is required.

Packet level QoS - Every multimedia service type can have a packet loss rate (PLR) requirement. Each packet also should be transmitted within a delay/time jitter bound for real-time multimedia applications, and throughput is a good QoS criterion.

Application-level QoS - Bit and packet level QoS may not directly reflect service quality perceived by the end user. In another word, application layer perceived QoS parameters are more suitable to represent the service seen by the end user, such as, the peak signal to noise ratio (PSNR) for video application, the end-to-end throughput

for data application, and mean square error (MSE)/structural similarity (SSIM) [52] for image application.

1.5 Contribution

This dissertation includes a general information sharing cross-layer design and two other topics that address QoS provision and energy efficiency in WSNs. Specific contributions are as follows:

- A cross-layer design for WSNs based on the MIMO techniques is proposed. Performance analysis and simulation results show that throughput and packet will have different performance compared with only considering the MIMO scheme in physical layer as the increase of the number of transmitters.
- We introduce a new method for cross-layer design. We applied the FLS to coordinate the physical layer, the data-link layer and the application layer for cross-layer design. Simulation results show that our cross-layer design can reduce the average delay, increase the throughput and extend the network lifetime. The network performance parameters could also keep stable after the cross-layer optimization. And we extended the FLS from type-1 to type-2. We apply type-2 to coordinate physical layer and data link layer. Simulation results show that the interval type-2 FLS performs much better than the type-1 FLS in transmission delay prediction. And FLSs performs better than back-prop NN.
- Existing WSNs provide only limited quality of service (QoS) for image application. Hence, We considered cross-layer design for image transmission in wireless sensor networks. We combine application layer, MAC layer and physical layer together for cross-layer design. Application level QoS was applied to evaluate the cross-layer design for WSNs.

- Latency and energy efficiency are two important parameters to evaluate the WSNs. In the first topic, the WSN had a cell-partitioned structure and the two-hop relay algorithm was adopted. The relay/destination nodes selection would determine the networks performance. The fuzzy logic system (FLS) is applied to the nodes selection. The output of FLS application provides a node election probability. In the second topic, the interference will affect the packets transmission. When a sensor needs to send a packet, we choose the parameter signal-to-interference ratio (SIR) as the threshold to decide whether send or not. SIR thresholds selection show SIR could manage the tradeoff between the average delay and energy consumption. We propose fuzzy logic system (FLS) in the optimization of SIR threshold selection. Simulation result show the fuzzy optimization could achieve a better network efficiency, reduce the average delay and extend the network lifetime.

1.6 Preliminories

1.6.1 Architecture of OSI Structure

Fig.1.1 shows the architecture of OSI Structure. The horizontal connectors are cross-layer interaction and the vertical connectors are strict layer interaction.

1.6.2 IEEE 802.11a OFDM PHY

The physical layer is the interface between the wireless medium and the MAC [14]. The principle of OFDM is to divide a high-speed binary signal to be transmitted over a number of low data-rate subcarriers. A key feature of the IEEE 802.11a PHY is to provide 8 PHY modes with different modulation schemes and coding rates, making the idea of link adaptation feasible and important, as listed in Table 1.1. BPSK, QPSK, 16-QAM and 64-QAM are the supported modulation schemes. The OFDM provides a

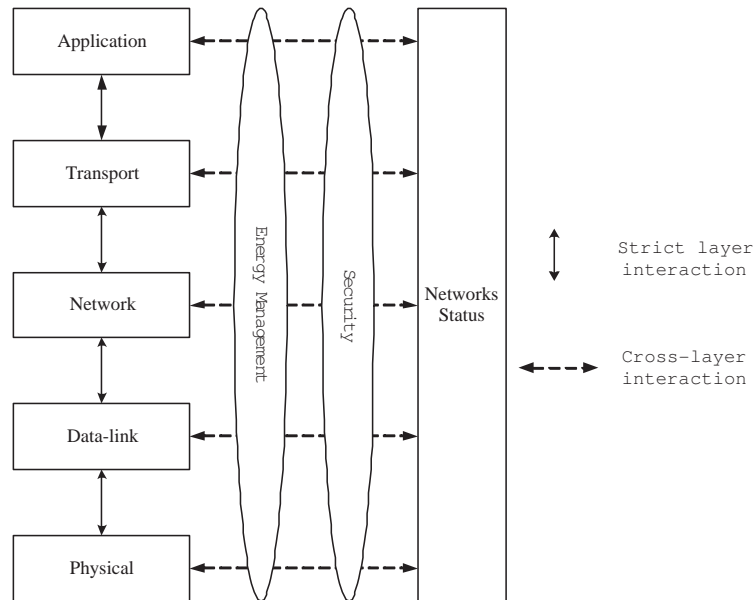


Figure 1.1. OSI Stack.

data transmission rates from 6 to 54MBPS. The higher code rates of $2/3$ and $3/4$ are obtained by puncturing the original rate $1/2$ code.

1.6.3 IEEE 802.11 MAC

The 802.11 MAC uses Carrier-Sense Multiple Access with Collision Avoidance (CSMA/CA) to achieve automatic medium sharing between compatible stations. In CSMA/CA, a station senses the wireless medium to determine if it is idle before it starts transmission. If the medium appears to be idle, the transmission may proceed, else the station will wait until the end of the in-progress transmission. A station will ensure that the medium has been idle for the specified inter-frame interval before attempting to transmit.

Besides carrier sense and RTS/CTS mechanism, an acknowledgment (ACK) frame will be sent by the receiver upon successful reception of a data frame. Only after receiving

Table 1.1. Eight PHY Modes of the IEEE802.11A PHY

| <i>Mode</i> | <i>Modulation</i> | <i>CodeRate</i> | <i>DataRate</i> | <i>BpS*</i> |
|-------------|-------------------|-----------------|-----------------|-------------|
| 1 | <i>BPSK</i> | 1/2 | 6Mbps | 3 |
| 2 | <i>BPSK</i> | 3/4 | 9Mbps | 4.5 |
| 3 | <i>QPSK</i> | 1/2 | 12Mbps | 6 |
| 4 | <i>QPSK</i> | 3/4 | 18Mbps | 9 |
| 5 | 16 – <i>QAM</i> | 1/2 | 24Mbps | 12 |
| 6 | 16 – <i>QAM</i> | 3/4 | 36Mbps | 18 |
| 7 | 64 – <i>QAM</i> | 2/3 | 48Mbps | 24 |
| 8 | 64 – <i>QAM</i> | 3/4 | 54Mbps | 27 |

*Bytes per OFDM Symbol

an ACK frame correctly, the transmitter assumes successful delivery of the corresponding data frame. The sequence for a data transmission is: RTS-CTS-DATA-ACK.

A mobile node will retransmit the data packet when finding failing transmission. Retransmission of a signal packet can achieve a certain probability of delivery. There is a relationship between the probability of delivery p and retransmission times n [15]:

$$n = 1.45 \ln \frac{1}{1-p} \quad (1.1)$$

The IEEE 802.11 standard requires that the transmitter's MAC discard a data frame after certain number of unsuccessful transmission attempts. According to the requirement of probability of delivery, we choose the minimum number of retransmission. The advantage is we can save energy through avoiding unnecessary retransmission, and ensure probability of delivery.

1.7 Network Layer

The Ad hoc On Demand Distance Vector (AODV) routing algorithm is a routing protocol designed for ad hoc mobile networks [16]. AODV is capable of both unicast and multicast routing. It is an on demand algorithm, meaning that it builds routes

between nodes only as desired by source nodes. It maintains these routes as long as they are needed by the sources. Additionally, AODV forms trees, which connect multicast group members. The trees are composed of the group members and the nodes needed to connect the members. AODV uses sequence numbers to ensure the freshness of routes. It is loop-free, self-starting, and scales to large numbers of mobile nodes.

AODV builds routes using a route request/route reply query cycle. As long as the route remains active, it will continue to be maintained. A route is considered active as long as there are data packets periodically traveling from the source to the destination along that path. Once the source stops sending data packets, the links will time out and eventually be deleted from the intermediate node routing tables. If a link break occurs while the route is active, the node upstream of the break propagates a route error (RERR) message to the source node to inform it of the now unreachable destination(s). After receiving the RERR, if the source node still desires the route, it can reinitiate route discovery.

Multicast routes are set up in a similar manner. AODV maintains routes for as long as the route is active. This includes maintaining a multicast tree for the life of the multicast group. Because the network nodes are mobile, it is likely that many link breakages along a route will occur during the lifetime of that route.

1.7.1 Application Layer

Traffic in application layer is divided into two classes: real-time and best-effort. Each node in the mobile ad hoc networks independently regulates best effort traffic. It is proposed to control the rate of the best-effort traffic to avoid excessive delays of the real-time traffic by using local per-hop delays as a feedback to local rate controller [8]. The general behavior of a congestion-controlled system is illustrated in Fig.1.2. The control algorithm ensures that the system operates around, or preferably close to the

”cliff”, which ensure maximum system throughput, but at the cost of large average packets delay. The control algorithm discussed, on the other hand, keep the system at the delay ”knee” where the system throughput is almost the same as the at the cliff, but the buffers are significantly less loaded, so the delay is close the minimum. Due to loss typically happens at the cliff, while delays start to increase at the knee, we use the per-hop MAC delay as a feedback for local control instead of the packet loss.

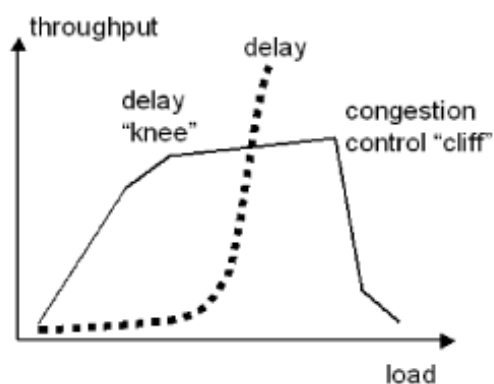


Figure 1.2. General Behavior of a Congestion-controlled System.

When MAC layer acquires access to the channel, the nodes will exchange the RTS-CTS-DATA-ACK packets. After the transmitters receive an ACK packet, a packet is transmitted successfully. The packet delay represents the time it took to send the packet between the transmitter and the next-hop receiver, including the deferred time and the time to fully acknowledge the packet. In this chapter, we assume that there will be always best-effort traffic present that can be locally and rapidly rate controlled in an independent manner at each node to yield necessary low delays and stable throughputs.

1.7.2 Energy

A mobile node consumes significant energy when it transmits or receives a packet. But we will not consider the energy consumed when the mobile node is idle.

The distance between two nodes are variable in the mobile ad hoc networks and the power loss model is used. To send the packet, the sender consumes [17],

$$P_{tx} = P_{elec} + \epsilon_{fs} \cdot d^2 \quad (1.2)$$

and to receive the packet, the receiver consumes,

$$P_{rx} = P_{elec} \quad (1.3)$$

where P_{elec} represents the power that is necessary for digital processing, modulation, and ϵ_{fs} represents the power dissipated in the amplifier for the free space distance d transmission.

A joint characteristic of most application scenarios of mobile ad hoc networks is that mobile nodes only have a limited energy supply which might not even be rechargeable, hence they have to be energy-efficient as possible. Transmitter power control allows interfering communication links sharing the same channel to achieve their required QoS levels, minimizing the needed power, mitigating the channel interference, and maximizing the network user/link capacity.

1.7.3 Delay

The packet transmission delay between the mobile nodes includes three parts: the wireless channel transmission delay, the Physical/MAC layer transmission delay, and the queuing delay [18] [19].

Defining D as the distance between two nodes and C as the light speed, the wireless channel transmission delay as:

$$Delay_{ch} = \frac{D}{C} \quad (1.4)$$

The Physical/MAC layer transmission delay will be decided by interaction of the transmitter and the receive channel, the node density and the node traffic intensity etc.

The queuing delay is decided by the mobile node I/O system-processing rate, the subqueue length in the node.

In order to make the system “stable”, the rate at which node transfers packets intended for its destination must satisfy all nodes that the queuing lengths will not be infinite and the average delays will be bounded.

1.7.4 Node Mobility and Channel Fading

Mobility of a mobile node generates a doppler shift, which is a key parameter of fading channel. The doppler shift is

$$f_d = \frac{v}{c} f_c \quad (1.5)$$

where v is the ground speed of a mobile node, c is the speed of light ($3 \times 10^8 m/s$), and f_c is the carrier. In our simulation, we used the carrier is $6GHz$. For reference, if a node moves with speed $10m/s$, the doppler shift is $200Hz$.

We model channel fading in ad hoc networks as Rayleigh fading. Rayleigh fading occurs when there is a strong specular (direct path or line of sight component) signal in addition to the scatter (multipath) components. For example, in communication between two infrared nodes, there exist a direct path. The channel gain,

$$g(t) = g_I(t) + jg_Q(t) \quad (1.6)$$

can be treated as a wide-sense stationary complex Gaussian random process, and $g_I(t)$ and $g_Q(t)$ are Gaussian random processes with zero means; and they have same variance σ^2 , then the magnitude of the received complex envelop has a Rayleigh distribution,

$$p_\alpha(x) = \frac{x}{\sigma^2} \exp\left\{-\frac{x^2}{2\sigma^2}\right\} \quad x \geq 0 \quad (1.7)$$

This kind of channel is known as Rayleigh fading channel. A Rayleigh channel is characterized by parameter, the Doppler spread (or single-sided fading bandwidth) f_d . The Rayleigh fade generator is based on Jakes' model [20] in which an ensemble of sinusoidal waveforms are added together to simulate the coherent sum of scattered rays with Doppler spread f_d arriving from different directions to the receiver.

BPSK, QPSK, 16-QAM and 64-QAM are the supported modulation schemes for IEEE 802.11a OFDM physical layer. We can show their performance curves with Rayleigh fading in Fig.1.3.

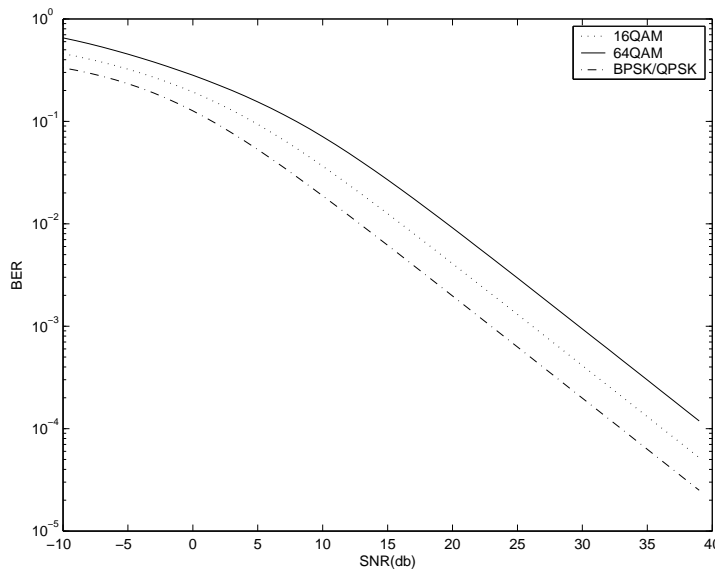


Figure 1.3. BER Curves with Rayleigh Fading and Different Modulation.

The BER performances are provided in Appendix A. After we introduce the channel coding and node mobility into the modulation schemes, the modulation curves will change a lot. For the same SNR, channel coding will improve the BER performance and the mobility will degrade the BER performance.

1.7.5 One-step Markov Path Model

The mobile nodes are roaming independently with variable ground speed. The mobility model is called one-step Markov path model [21]. The probability of moving in the same direction as the previous move is higher than other directions in this model, which means this model has memory. Fig.1.4 shows the probability of the six directions.

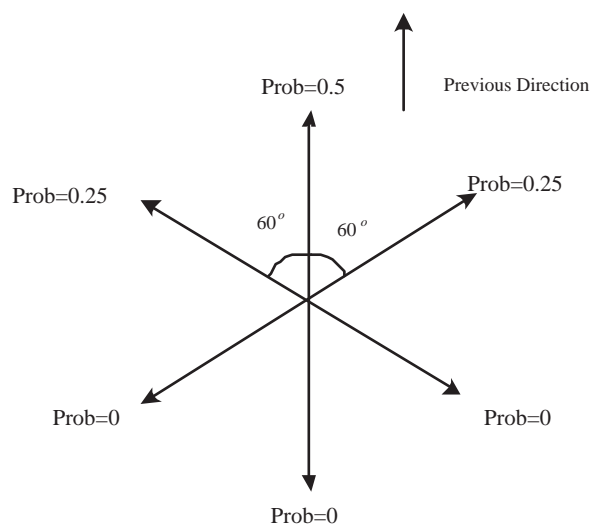


Figure 1.4. One-step Markov Path Model.

1.8 Dissertation Structure

The remainder of this dissertation is structured as following. In chapter 2, we introduce cross-layer design for WSNs Based on the MIMO techniques. In chapter 3,

bottom-up cross-layer optimization for mobile ad hoc networks is introduced. In chapter 4, we make an introduction of cross-layer design for mobile ad hoc networks using interval type-2 FLS. In chapter 5, we introduce cross-layer design for image transmission in WSNs. In chapter 6, latency-aware and energy efficiency tradeoffs for WSNs is introduced. Packets transmission in WSNs: interference, energy and delay-aware approach is presented in chapter 7. In chapter 8, we conclude the dissertation.

CHAPTER 2

CROSS-LAYER DESIGN FOR WSNS BASED ON MIMO TECHNIQUES

2.1 Introduction

MIMO systems can support higher data rate under the same transmit power budget and bit-error-rate performance requirement as single-input-single-output (SISO) systems. However, direct application of multi-antenna techniques to sensor networks is impractical due to the limited physical size of a sensor node that is typically can only support a single antenna. Fortunately, if we allow individual single-antenna nodes to cooperate on information transmission and/or reception, a cooperative MIMO system can be constructed such that energy efficient MIMO scheme can be deployed [22] [23].

Using cooperative MIMO, we show that the end-to-end performance can be dramatically improved. Moreover, the novel approach of distributed Alamouti [24] coding provides diversity gain with no local information exchange, as is typically required in node cooperation.

However, the routing and MAC layer protocols have different effects on network performance compared with cooperative MIMO technique. Performance analysis and simulation results have been illustrated this situation

The remainder of this chapter is structured as following. In Section 2.2, we introduce the preliminaries. In Section 2.3, we make the performance analysis for all the layers. In Section 2.4, we make the performance analysis for cross-layer model. Simulation results and discussions are presented in Section 2.5. In Section 2.6, we conclude the chapter.

2.2 Preliminaries

2.2.1 IEEE 802.11a OFDM PHY

The physical layer is the interface between the wireless medium and the MAC [14]. The principle of OFDM is to divide a high-speed binary signal to be transmitted over a number of low data-rate subcarriers. A key feature of the IEEE 802.11a PHY is to provide 8 PHY modes with different modulation schemes and coding rates, making the idea of link adaptation feasible and important. BPSK, QPSK, 16-QAM and 64-QAM are the supported modulation schemes. The OFDM provides a data transmission rates from 6 to 54MBPS. The higher code rate of 2/3 and 3/4 are obtained by puncturing the original rate 1/2 code.

2.2.2 IEEE 802.11 MAC

The 802.11 MAC uses Carrier-Sense Multiple Access with Collision Avoidance (CSMA/CA) to achieve automatic medium sharing between compatible stations. In CSMA/CA, a station senses the wireless medium to determine if it is idle before it starts transmission. If the medium appears to be idle, the transmission may proceed, else the station will wait until the end of the in-progress transmission. A station will ensure that the medium has been idle for the specified inter-frame interval before attempting to transmit.

A mobile node will retransmit the data packet when finding failing transmission. Retransmission of a signal packet can achieve a certain probability of delivery. There is a relationship between the probability of delivery p and retransmission times n [15]:

$$n = 1.45 \ln \frac{1}{1-p} \quad (2.1)$$

The IEEE 802.11 standard requires that the transmitter's MAC discard a data frame after certain number of unsuccessful transmission attempts. According to the

requirement of probability of delivery, we choose the minimum number of retransmission. The advantage is that we can save energy through avoiding unnecessary retransmission, and ensure probability of delivery.

2.2.3 Network Layer

AODV is capable of both unicast and multicast routing [16]. It is an on demand algorithm, means that it builds routes between nodes only as desired by source nodes. It maintains these routes as long as they are needed by the sources. Additionally, AODV forms trees that connect multicast group members. The trees are composed of the group members and the nodes needed to connect the members. AODV uses sequence numbers to ensure the freshness of routes. It is loop-free, self-starting, and scales to large numbers of mobile nodes.

2.2.4 Node Mobility and Channel Fading

Mobility of a mobile node generates a doppler shift, which is a key parameter of fading channel. The doppler shift is

$$f_d = \frac{v}{c} f_c \quad (2.2)$$

where v is the ground speed of a mobile node, c is the speed of light ($3 \times 10^8 m/s$), and f_c is the carrier. In our simulation, we used the carrier is $6GHz$. For reference, if a node moves with speed $10m/s$, the doppler shift is $200Hz$.

We model channel fading in wireless sensor networks as Rayleigh fading. Rayleigh fading occurs when there is a strong specular (direct path or line of sight component) signal in addition to the scatter (multipath) components. For example, in communication between two infrared nodes, there exist a direct path. The channel gain,

$$g(t) = g_I(t) + jg_Q(t) \quad (2.3)$$

can be treated as a wide-sense stationary complex Gaussian random process, and $g_I(t)$ and $g_Q(t)$ are Gaussian random processes with zero means; and they have same variance σ^2 , then the magnitude of the received complex envelop has a Rayleigh distribution,

$$p_\alpha(x) = \frac{x}{\sigma^2} \exp\left\{-\frac{x^2}{2\sigma^2}\right\} \quad x \geq 0 \quad (2.4)$$

This kind of channel is known as Rayleigh fading channel. A Rayleigh channel is characterized by parameter, the Doppler spread (or single-sided fading bandwidth) f_d . The Rayleigh fade generator is based on Jakes' model [20] in which an ensemble of sinusoidal waveforms are added together to simulate the coherent sum of scattered rays with Doppler spread f_d arriving from different directions to the receiver.

For the values of M for MPSK(Mary phase shift keying), one can use the approximate BER expression obtained by Lu et al [25]. For the AWGN(Additive white Gaussian noise), which is accurate for a wide range of SNRs, again making the substitution $\gamma \log_2 M$ for E_b/N_0 followed by averaging over the PDF of γ . Using the alternative form of the Gaussian Q-function, it is straightforward to show that the result of the evaluation is given by:

$$P_b(E) \cong \frac{2}{\max(\log_2 M, 2)} \sum_{i=1}^{\max(\frac{M}{4}, 1)} \frac{1}{\pi} \times \int_0^{\frac{\pi}{2}} M_\gamma\left(-\frac{1}{\sin^2 \theta} \frac{E_b \log_2 M}{N_0} \sin^2 \frac{(2i-1)\pi}{M}\right) d\theta \quad (2.5)$$

where $M_\gamma(s)$ is the MGF(Moment generating function)of the instantaneous fading power γ . For a Rayleigh fading channel, we obtain the following analogous to:

$$P_b(E) \cong \frac{1}{\max(\log_2 M, 2)} \sum_{i=1}^{\max(\frac{M}{4}, 1)} \left(1 - \sqrt{\frac{\frac{E_b \log_2 M}{N_0} \sin^2 \frac{(2i-1)\pi}{M}}{1 + \frac{E_b \log_2 M}{N_0} \sin^2 \frac{(2i-1)\pi}{M}}}\right) \quad (2.6)$$

For BPSK, we get the result:

$$P_b(E) \cong \frac{1}{2} \left(1 - \sqrt{\frac{\frac{E_b}{N_0}}{1 + \frac{E_b}{N_0}}}\right) \quad (2.7)$$

2.3 Performance Analysis

2.3.1 MIMO

It is widely understood that in a system with multiple transmit and receive antennas, the spectral efficiency is much higher than that of the conventional single-antenna channels, i.e., a MIMO system can provide two types of gains: diversity gain and multiplexing gain.

2.3.1.1 MIMO Diversity Gain

The multiple antennas at the transmitter and receiver can be used to obtain diversity gain: This scheme is also referred to as MIMO beam forming [26] [27].

Two-Branch transmit diversity with one receiver: the scheme uses two transmit antennas and one receive antenna and may be defined by the following three functions: the encoding and transmission sequence of information symbols at the transmitter; the combining scheme at the receiver; the decision rule for maximum likelihood detection.

The encoding and transmission sequence: at a given symbol period, two signals are simultaneously transmitted from the two antennas. The signal transmitted from antenna zero is denoted by c_1 and from antenna one by c_2 . During the next symbol period signal $-c_2^*$ is transmitted from antenna zero, and signal c_1^* is transmitted from antenna one where $*$ is the complex conjugate operation.

$$r_1 = h_1 c_1 + h_2 c_2 + n_1 \quad (2.8)$$

$$r_2 = -h_1 c_2^* + h_2 c_1^* + n_2 \quad (2.9)$$

where r_1 and r_2 are the received signals at time t and $t+T$ and n_1 and n_2 are complex random variables representing receiver noise and interference.

We will build the following two combined signals that are sent to the maximum likelihood detector:

$$\tilde{c}_1 = (\alpha_1^2 + \alpha_2^2)c_1 + h_1^*n_1 + h_1n_2^* \quad (2.10)$$

$$\tilde{c}_2 = (\alpha_1^2 + \alpha_2^2)c_2 + h_1n_2^* + h_1^*n_1 \quad (2.11)$$

The combined signals are then sent to the maximum likelihood detector, uses the decision rule to decide the signals c_1 or c_2 .

It is further shown that the scheme may easily be generalized to M transmit antennas and one receive antenna to provide diversity gain M.

2.3.1.2 MIMO Multiplexing Gain

One mechanism for utilizing to improve wireless system performance is to obtain gain by decomposing the MIMO channel into parallel channels and multiplexing different data streams onto these channels. By multiplexing independent data onto these independent channels, we get an increase in data rate in comparison to a system with just one antenna at the transmitter and receiver. This increased data rate is called multiplexing gain.

2.3.1.3 MIMO Diversity-Multiplexing Gain Tradeoffs

The MIMO diversity-multiplexing gain tradeoffs are essentially the tradeoff between the error probability and the data rate of a system.

A scheme(SNR)is said to achieve spatial multiplexing gain r and diversity gain d if the data rate [28]:

$$\lim_{SNR \rightarrow \infty} \frac{R(SNR)}{\log SNR} = r \quad (2.12)$$

and the average error probability

$$\lim_{SNR \rightarrow \infty} \frac{\log P_e(SNR)}{\log SNR} = -d \quad (2.13)$$

For each r , the optimal diversity gain $d_{opt}(r)$ is maximum diversity gain that can be achieved by any scheme.

$$d_{opt}(r) = (M_t - r)(M_r - r) \quad (2.14)$$

$$0 \leq r \leq \min(M_t, M_r) \quad (2.15)$$

Equation(2.14)(2.15) are plotted in Fig.2.1.

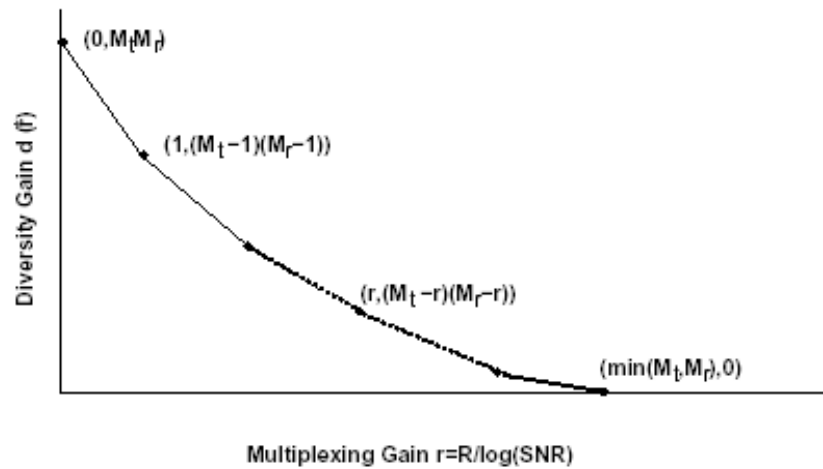


Figure 2.1. Diversity-multiplexing trade-offs.

This figure implies if we use all transmit and receive antennas for diversity then we get full diversity gain $M_t M_r$, and we can use some of these antennas to increase data rate at the expense of diversity gain.

2.3.2 IEEE 802.11 MAC Protocol

Assuming that there are n sensor nodes in the wireless LAN we are considering, and p_c is the probability of a collision seen by a packet being transmitted on the medium [29] [30] [31]. We observe that p_c is also the probability that there is at least one

packet transmission in the medium among other $(n-1)$ nodes in the interference range of the node under consideration. This yields:

$$p_c = 1 - [1 - (1 - p_0)\tau]^{n-1} \quad (2.16)$$

where p_0 is the probability that there is no packet ready to transmit at the MAC layer in sensor node under consideration, and τ is the packet transmission probability that the node transmits in a randomly chosen slot time given that the station has packets to transmit at the MAC layer. In non-saturated scenario, p_c mainly depends on the total number of packets attempting to transmit by all neighboring nodes. However, in saturated scenario, i.e. the stations always have packets to transmit, the total number of packets attempting to transmit equals to the total number of neighboring nodes, hence p_c is mainly dependent on the total number of neighboring nodes.

The service time distribution and the arrival process in addition to the service discipline can characterize a queue model. In this chapter, we assume that the packet arrivals at each sensor node follow the Poisson process or a deterministic distribution with average arrival rate λ . The packet transmission process at each node can be modeled as a general single server. The buffer size at each node is K . Thus the queuing model for each node can be modeled as an M/G/1/K when Poisson arrivals of packets are assumed.

Let p_n represent the steady-state probability of n packets in the queuing system, and let π_n represent the probability of n packets in the queuing system upon a departure at the steady state, λ' is the average arrival rate, \overline{T}_s is the duration of time taken for a state transition from the start state (beginning to be served) to the end state (being transmitted successfully or discarded after maximum α times retransmission failures), ρ is the traffic intensity $\rho = \lambda'\overline{T}_s$. For the finite system size K with Poisson input [32], we have

$$p_0 = \frac{p_0}{\pi_0 + \rho} \quad (2.17)$$

$$p_n = \frac{p_n}{\pi_0 + \rho} \quad (2.18)$$

$$p_K = 1 - \frac{1}{\pi_0 + \rho} \quad (2.19)$$

The average queue length, blocking probability, and average waiting time including MAC service time are given by,

$$L = \sum_{i=0}^K i \times p_i \quad (2.20)$$

$$p_b = 1 - \frac{1}{\pi_0 + \rho} \quad (2.21)$$

$$W = \frac{L}{\lambda(1 - p_b)} \quad (2.22)$$

If we know the blocking probability p_b , then the throughput S can be computed easily by:

$$S = (1 - p_b)(1 - p_c^{\alpha+1}) \quad (2.23)$$

where α is the maximum retransmission times, $p_c^{\alpha+1}$ is the packet discard probability due to transmission failure.

Suppose α is constant, as n increases, p_c increases, then the packet discarding probability at MAC layer increases.

Throughput linearly increases with the offered load at the non-saturated status and maintains a constant value with different total number of transmitting nodes at the saturated status. As the n increases, the constant value decreases.

2.3.3 AODV Routing Protocol

Using the OPnet and NS-2, we could conduct an extensive set of performance experiments for the AODV routing protocol [33] [34] [35].

1. With the increase of number of hops, throughput degrades due to the higher delay.

2. With the increase of loads (i.e. application traffic), throughput can again be degraded due to the loss at the link layer. Link layer losses could be due to problems of hidden/exposed node or collisions in wireless media.
3. The connectivity between nodes decreases, throughput also decreases.
4. The mobility increases, throughput decreases.

2.4 Cross-layer Analysis

When we combine the physical layer, the MAC layer and the network layer, we need to analyze two performance parameters: throughput and packet loss ratio (PLR).

2.4.1 Throughput

According to the performance analysis of the physical layer, MIMO scheme could achieve multiplexing gain to increase the throughput as the number of transmitters increases.

For the CSMA/CA MAC protocol, in non-saturated scenario, throughput linearly increases with the offered load, i.e., the throughput will increase. As the number of transmitters increases, it will be the saturated scenario. The throughput will decrease as the number of transmitters increases.

For AODV routing protocol, the number of transmitters increases, the more routing paths are set up, and the throughput increases. However, as more routing paths are setting up, the connectivity between nodes decreases, throughput decreases.

For cross-layer analysis, we can conclude: as the number of transmitters increases, the throughput will increase. When the number is large enough, the MAC and AODV routing protocol will have inverse effects on throughput compared with that of MIMO scheme.

2.4.2 Packet Loss Ratio

MIMO scheme could achieve diversity gain to increase the performance as the number of transmitters increases. So the BER will decrease. If each bit inside the L length packet has the same BER and bit-errors are uncorrelated, the PER can be related to the BER through [7]:

$$PER = 1 - (1 - BER)^L \quad (2.24)$$

We could conclude that for MIMO scheme, the PER will decrease as the number of transmitters increase.

For CSMA/CA MAC protocol, as the number of transmitter increases, the total number of packets attempt to transmit will increase, the collision probability will increase. Suppose the maximum retransmission times is constant, the packet discard probability $p_c^{\alpha+1}$ will increase .

In AODV routing protocol, the node density keeps unchanged as the increase of the number of the transmitters. It is hard to establish enough routing paths. The buffer size in each sensor node is constant, the arriving packets rate is constant, and more packets will be discarded when the buffer is full.

For cross-layer analysis, we can conclude: as the number of transmitters increases, the PLR will decrease. However, PLR will increase as the MAC layer and the network layer will have larger effect on PLR than that of MIMO scheme.

2.5 Simulations and Analysis

Fig.2.2 illustrates the system architecture for cross-layer design. Only the source sensor nodes send out the packets. The source sensor nodes need to set up paths to the destination sensor node. There are three phases during the packets transmissions.

1. MIMO scheme for physical layer.

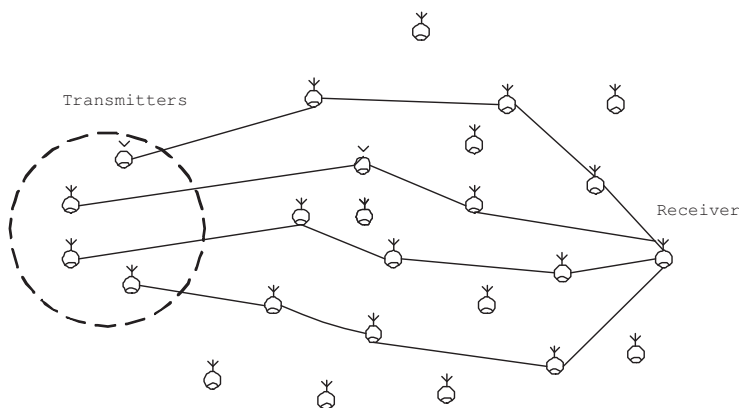


Figure 2.2. System Architecture for cross-layer design.

2. setting up the link in MAC layer.
3. routing path discovery in network layer.

We use Matlab to obtain the BER-SNR curves for MIMO schemes. We run 1000 Monte-Carlo simulations to get the physical layer curves.

We implemented the cross-layer model using the OPNET modeler. The simulation region is 1000×1000 meters. The wireless communication range is 300 meters. There were 49 mobile nodes in the simulation model, and the nodes were roaming independently with variable ground speed between 0 to 10 meters per second. The mobility model was called billiard mobility model. The maximum retransmission times are 7 and arriving packet distribution is Poisson. The modulation scheme is BPSK.

2.5.1 Throughput

Fig.2.3 is the throughput performance for the cross-layer model. It shows the throughput is maximized when the number of transmitters is 11. As the number of transmitters increases, throughput will increase for the MIMO scheme. For the MAC layer, when the number of transmitters is small, it is the non-saturated scenario. As the number of transmitters increases, throughput will increase. When the number of

transmitters is large enough, it is the saturated scenario. As the number of transmitters increases, throughput will decrease. For AODV protocol, the collision probability will increase as the number of transmitters increases. The simulation result is consented with the analysis result.

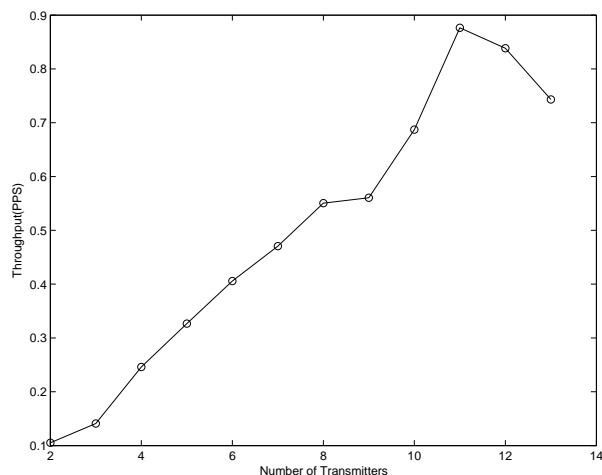


Figure 2.3. Throughput Vs Number of Transmitters.

2.5.2 Packet Loss Ratio

Fig.2.4 is the packet loss rate performance for the cross-layer model. The change of curve in Fig.2.4 is monotonous, and the best performance for PLR was achieved when the number of transmitter is 10. For MIMO scheme, as the number of transmitters increases, BER decreases, so PER decreases, more packets will be discarded, PLR decreases. For MAC layer protocol, when the number of transmitters increases, the probability of collision will increase. The packet loss ratio will keep stable for retransmission could solve the collision problem. If the number of transmitters is big enough, retransmission number will exceed the maximum retransmission number α , large number of packets will be discarded, the PLR will increase sharply. For AODV protocol, as the increase of the number

of transmitters, it is hard to set up enough routing paths. Large number of packets will jam in the finite-size buffer, so more packets will be discarded. The simulation result matched well with the performance analysis.

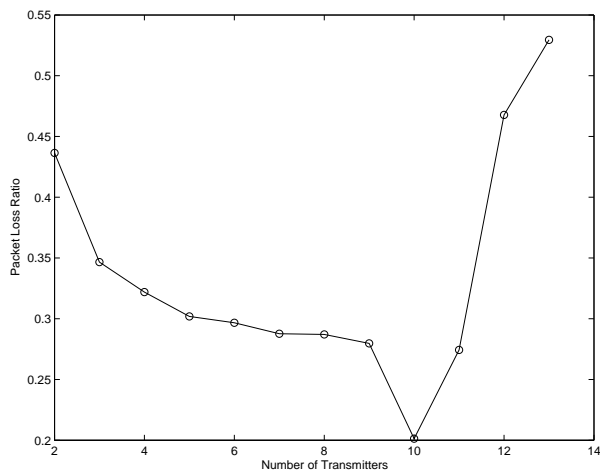


Figure 2.4. PLR Vs Number of Transmitters.

2.6 Conclusion and Analysis

MIMO scheme is an effective method to improve the performance of the WSNs. We applied the cross-layer evaluation to combine the physical layer, the MAC layer and the network layer together. According to the analysis and simulation, throughput and packet loss ratio performance will have different results compared with only considering the MIMO scheme in physical layer as the increase of the number of transmitters.

CHAPTER 3

BOTTOM-UP CROSS-LAYER OPTIMIZATION FOR MANET

3.1 Introduction

In this chapter, we propose to use the Fuzzy Logic System (FLS) in the cross-layer design. We define a coherent time, a certain period of time. During this coherent time, the AMC (Adaptive Modulation and Coding), transmission power, retransmission times and rate control decision are used for packet transmission. After this time, we adaptively adjust these parameters by FLS again basing on current ground speed, average delay and the packets successful transmission ratio. By applying the FLS mechanism to the cross-layer design, a better QOS provision and energy efficiency are achieved [36] [37].

3.2 Overview of Fuzzy Logic Systems

Figure 3.1 shows the structure of a fuzzy logic system (FLS).

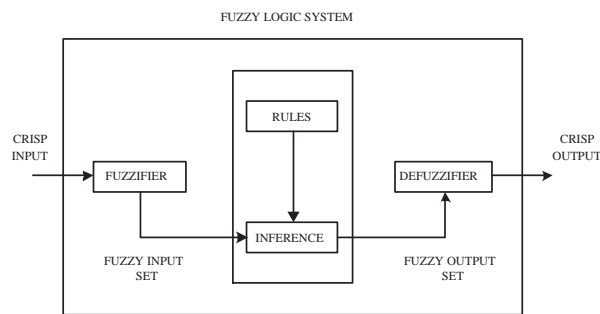


Figure 3.1. The structure of a fuzzy logic system.

When an input is applied to a FLS, the inference engine computes the output set corresponding to each rule. The defuzzifier then computes a crisp output from these

rule output sets [38]. Consider a p -input 1-output FLS, using singleton fuzzification, *center-of-sets* defuzzification [39] and “IF-THEN” rules of the form [40]

$$R^l : \text{IF } x_1 \text{ is } F_1^l \text{ and } x_2 \text{ is } F_2^l \text{ and } \dots \text{ and } x_p \text{ is } F_p^l, \text{ THEN } y \text{ is } G^l.$$

Assuming singleton fuzzification, when an input $\mathbf{x}' = \{x'_1, \dots, x'_p\}$ is applied, the degree of firing corresponding to the l th rule is computed as

$$\mu_{F_1^l}(x'_1) \star \mu_{F_2^l}(x'_2) \star \dots \star \mu_{F_p^l}(x'_p) = \mathcal{T}_{i=1}^p \mu_{F_i^l}(x'_i) \quad (3.1)$$

where \star and \mathcal{T} both indicate the chosen t -norm. There are many kinds of defuzzifiers. In this chapter, we focus, for illustrative purposes, on the center-of-sets defuzzifier. It computes a crisp output for the FLS by first computing the centroid, c_{G^l} , of every consequent set G^l , and, then computing a weighted average of these centroids. The weight corresponding to the l th rule consequent centroid is the degree of firing associated with the l th rule, $\mathcal{T}_{i=1}^p \mu_{F_i^l}(x'_i)$, so that

$$y_{cos}(\mathbf{x}') = \frac{\sum_{l=1}^M c_{G^l} \mathcal{T}_{i=1}^p \mu_{F_i^l}(x'_i)}{\sum_{l=1}^M \mathcal{T}_{i=1}^p \mu_{F_i^l}(x'_i)} \quad (3.2)$$

where M is the number of rules in the FLS.

3.3 Fuzzy Application For Cross-layer Design

AMC, transmission power, retransmission times and rate control decision will manage the energy consumption and QoS provision. How to choose a proper adjusting factor for these parameters will determine the wireless ad hoc networks performance.

We collect the knowledge for adjusting factor selection based on the following three antecedents:

1. Antecedent 1. Ground speed.
2. Antecedent 2. Average delay.
3. Antecedent 3. Packets successful transmission ratio.

The linguistic variables used to represent the ground speed, average delay and packets successful transmission ratio were divided into three levels: *low*, *moderate*, and *high*. The consequents – the adjusting factor for the AMC, transmission power, retransmission times and rate control decision were divided into 9 levels, *decrease three*, *decrease two*, *decrease one*, *unchanged*, *increase one*, *increase two*, *increase three*. Fig.3.2 show the FLS application for the cross-layer design.

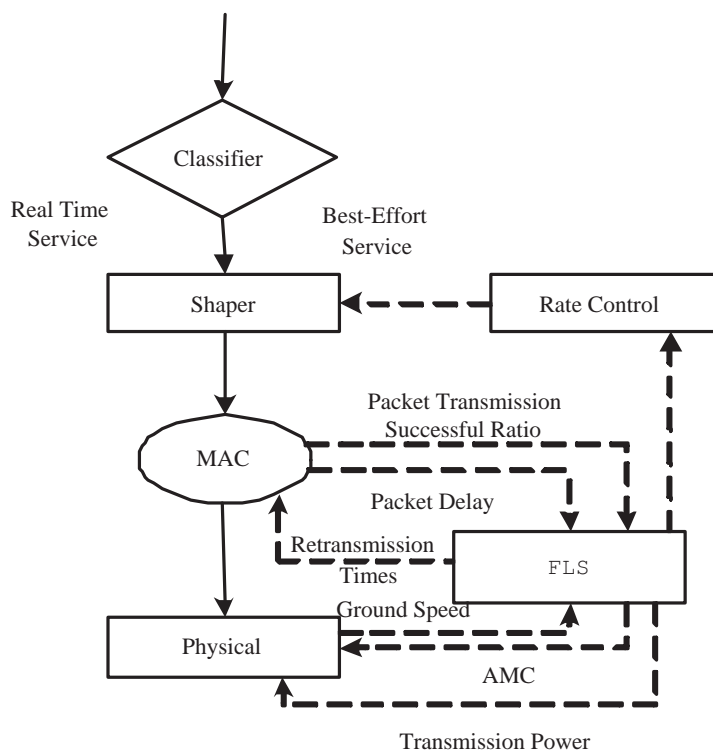


Figure 3.2. Cross-layer Design Algorithm.

We designed questions such as:

IF *ground speed* is *low*, *average delay* is *low* and *packets successful transmission ratio* is *high*, THEN the adjusting factor is _____.

So we need to set up $3^3 = 27$ (because every antecedent has 3 fuzzy sub-sets, and there are 3 antecedents) rules for this FLS. According the analysis in section 2, if

ground speed is high, we increase the adjusting factor for retransmission times, decrease the adjusting factor for AMC, increase the adjusting factor for transmission power and increase the adjusting factor for rate control decision. If average delay is high, we decrease the adjusting factor for retransmission times, increase the adjusting factor for AMC, increase the adjusting factor for transmission power and increase the adjusting factor for rate control decision. If packets successful transmission ratio is high, we decrease the adjusting factor for retransmission times, increase the adjusting factor for AMC, decrease the adjusting factor for transmission power and decrease the adjusting factor for rate control decision. Similar rules can be obtained for other cases. We summarized these rules in Table 3.1.

We used trapezoidal membership functions (MFs) to represent *low*, *high*, *increase four* and *decrease four*; and triangle MFs to represent *moderate*, *unchanged*, *increase one*, *increase two*, *increase three*, *decrease one*, *decrease two* and *decrease three*. We show these MFs in Fig.3.3 and Fig.3.4.

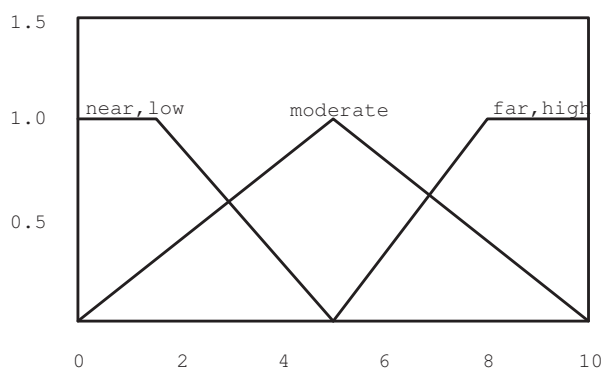


Figure 3.3. MFs for antecedents.

In our approach to form a rule base, we chose a single consequent for each rule. We designed a fuzzy logic system using rules such as:

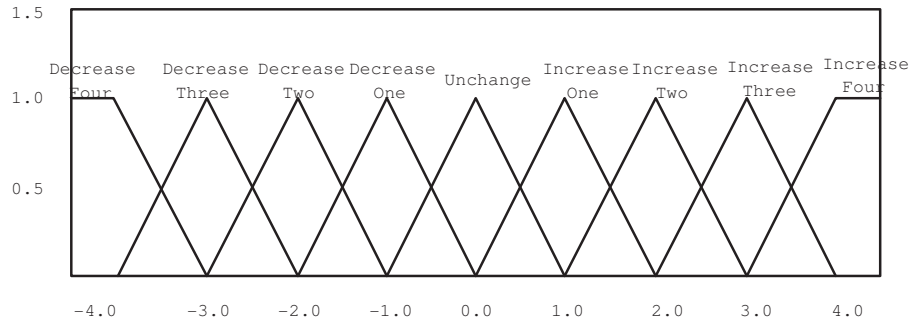


Figure 3.4. MFs for consequents.

R^l : IF *ground speed* (x_1) is F_l^1 , *average delay* (x_2) is F_l^2 , and *packets successful transmission ratio* (x_3) is F_l^3 , THEN the adjusting factor (y) is c^l .

For every input (x_1, x_2, x_3) , the output is computed using

$$y(x_1, x_2, x_3) = \frac{\sum_{l=1}^{27} \mu_{F_l^1}(x_1) \mu_{F_l^2}(x_2) \mu_{F_l^3}(x_3) c_G^l}{\sum_{l=1}^{27} \mu_{F_l^1}(x_1) \mu_{F_l^2}(x_2) \mu_{F_l^3}(x_3)} \quad (3.3)$$

We apply (3.3) to compute the adjusting factors and adjust the network parameters dynamically. Comparing to the constant parameters, the fuzzy optimization for cross-layer design can meet QoS and energy requirement.

3.4 Simulations

We implemented the simulation model using the OPNET modeler. The simulation region is 300×300 meters. There were 12 mobile nodes in the simulation model, and the nodes were roaming independently with variable ground speed between 0 to 10 meters per second. The mobility model was called one-step Markov path model. The movement would change the distance between mobile nodes.

3.4.1 Average Delay

Because data communications in the mobile networks have trimming constraints, it is important to design the network algorithm to meet a kind of end-end deadline [41]. We used the average delay to evaluate the network performance.

$$d_{average} = \frac{\sum_{i=1}^k d_i}{k} \quad (3.4)$$

Each packet was labeled a timestamp when it was generated by the source mobile node. When its destination mobile node received it, the time interval was the transmission delay.

Fig.3.5 showed the delay performance of the constant parameters and the one after cross-layer optimization for the real time traffic, the best effort traffic and all the traffic. Cross-layer optimization made a tradeoff for the average delay between the real time traffic and the best effort traffic. For the real time traffic, the cross-layer optimization would enlarge about 2.0 seconds. However for the best effort case, the cross-layer optimization could reduce the delay by up to 86.74%. For the all traffic, the cross-layer optimization could reduce the delay by up to 45.73%, which meant the cross-layer optimization could improve the average delay performance for the whole system. As showed in the best effort case, the cross-layer optimization could make the average delay "stable", which was important for the communication system design.

3.4.2 Energy Efficiency

It is not convenient to recharge the battery, so the energy efficiency is extremely important for mobile ad hoc networks. The network should keep an enough number of "live" mobile nodes to collect data, which means the network need to keep the energy among the mobile nodes in balance. We used the remaining alive nodes as the parameter of the energy efficiency.

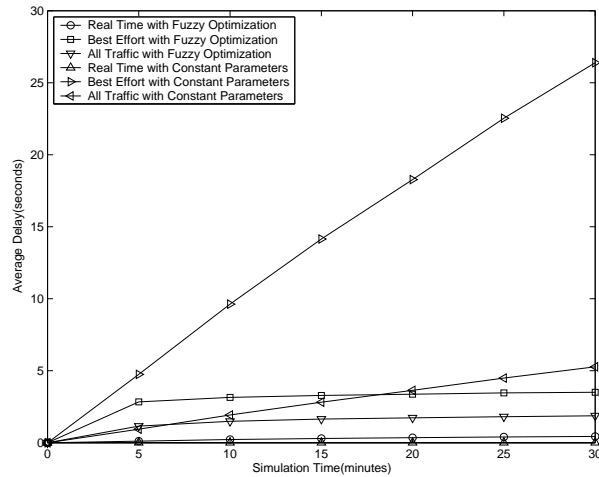


Figure 3.5. The Average Delay Versus Simulation Times.

The fuzzy computing consumed energy. In [42], we knew the energy consumed by computing was far less than that consumed by communication. We could only consider the communication energy consumption for energy efficiency.

In (1.2) and (1.3), we assumed P_{elec} was equal to 6.0×10^{-4} and ϵ_{fs} was equal to 6.0×10^{-4} . We assumed that the energy of each mobile node was 0.07 J.

When the remaining energy of a mobile node was lower than a certain threshold, the node was considered as “dead”. In this simulation, we chose 1.2×10^{-3} as the threshold. A sensor was “dead” meant it could not transmit/receive packets any longer, so it would be ignored by network. The number of nodes of mobile ad hoc networks, which was below a certain threshold means this network, does not work.

As Fig.3.6 showed, after fuzzy optimization, the duration of the first node “dead” is 1.5 times longer than that of the constant parameters, which is 1404 seconds.

3.4.3 Network Efficiency

The mobile ad hoc networks were used to collect data and transfer packets. The throughput of packets transmitted was one of the parameters to evaluate the networks

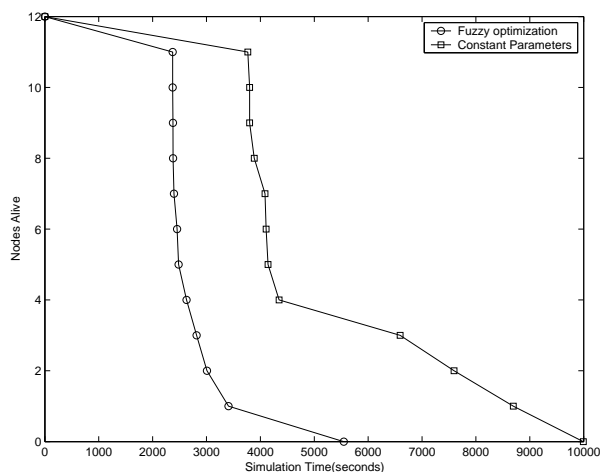


Figure 3.6. Number of Nodes Alive Versus Simulation Time.

efficiency. In our simulation, we assumed the collecting data distribution of the mobile node was Poisson distribution and the arriving interval was 0.2 second. Observe Fig.3.7, the cross-layer optimization made a tradeoff between the real time traffic and the best effort traffic. For the real time traffic, after the cross-layer optimization, the throughput of the network was about 0.02% smaller than that of the constant parameters. However, for the best effort traffic, the throughput of the network was up to 59.19% larger. For the all the traffic case, after the cross-layer optimization, the throughput of the network was up to 27.73% larger, which meant the cross-layer optimization could improve the throughput performance for the whole system. Same as the performance of the average delay, the cross-layer optimization could achieve a "stable" throughput performance.

We introduced the fuzzy logic system in the cross-layer design. Compare with other algorithms for cross-layer design, the fuzzy method could be flexible and simpler to implement and the performance outputs are also impressive.

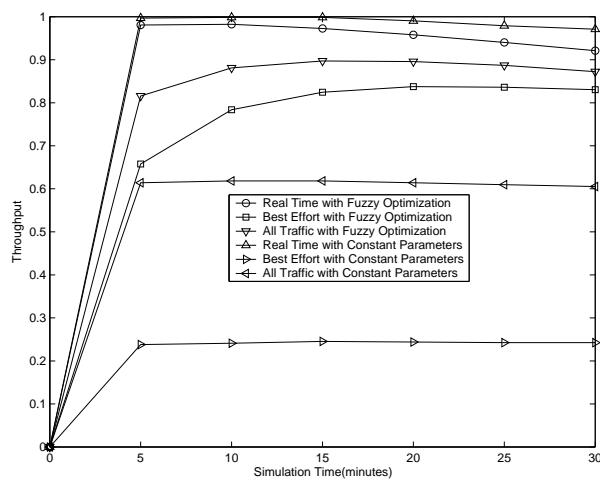


Figure 3.7. Throughput Versus Simulation Time.

3.5 Conclusions

Cross-layer design is an effective method to improve the performance of the mobile ad hoc network. We applied the FLS to combine the physical layer, the data-link layer and the application layer together. We selected ground speed, average delay and packets transmission successful ratio as antecedents. The output of FLS provides adjusting factors for the AMC, transmission power, retransmission times and rate control decision. Simulation showed the FLS application in cross-layer design could reduce the average delay, increase the throughput and extend the network lifetime. After the cross-layer optimization, the network performance parameters could also keep stability. In the future, We can consider other layers, such as network layer for the cross-layer design.

Table 3.1. The fuzzy rules for cross-layer design

Antecedent 1 is *its ground speed*, Antecedent 2 is *its average delay* and Antecedent 3 is *its packets successful transmission ratio*.

Consequent 1 is *adjusting factor for retransmission times*, Consequent 2 is *adjusting factor for AMC*, Consequent 3 is *adjusting factor for transmission power* and Consequent 4 is *adjusting factor for rate control decision*.

In this table, A stands for Antecedent, C stands for Consequent, u stands for unchanged, i stands for increase, and d stands for decrease.

| # | A 1 | A 2 | A 3 | C 1 | C 2 | C 3 | C 4 |
|----|----------|----------|----------|---------|---------|---------|---------|
| 1 | low | low | low | i two | d two | u | u |
| 2 | low | low | moderate | u | u | d two | d two |
| 3 | low | low | high | d two | i two | d four | d four |
| 4 | low | moderate | low | i one | d one | i one | i one |
| 5 | low | moderate | moderate | d one | i one | d one | d one |
| 6 | low | moderate | high | d three | i three | d three | d three |
| 7 | low | high | low | u | u | i two | i two |
| 8 | low | high | moderate | d two | i two | u | u |
| 9 | low | high | high | d four | i four | d two | d two |
| 10 | moderate | low | low | i three | d three | i one | i one |
| 11 | moderate | low | moderate | i one | d one | d one | d one |
| 12 | moderate | low | high | d one | i one | d three | d three |
| 13 | moderate | moderate | low | i two | d two | i two | i two |
| 14 | moderate | moderate | moderate | u | u | u | u |
| 15 | moderate | moderate | high | d two | i two | d two | d two |
| 16 | moderate | high | low | i one | d one | i three | i three |
| 17 | moderate | high | moderate | d one | i one | i one | i one |
| 18 | moderate | high | high | d three | i three | d one | d one |
| 19 | high | low | low | i two | d four | i two | i two |
| 20 | high | low | moderate | i two | d two | u | u |
| 21 | high | low | high | u | u | d two | d two |
| 22 | high | moderate | low | i three | d three | i three | i three |
| 23 | high | moderate | moderate | i one | d one | i one | i one |
| 24 | high | moderate | high | d one | i one | d one | d one |
| 25 | high | high | low | i two | d two | i four | i four |
| 26 | high | high | moderate | u | u | i two | i two |
| 27 | high | high | high | d two | i two | u | u |

CHAPTER 4

CROSS-LAYER DESIGN FOR MOBILE AD HOC NETWORKS USING INTERVAL TYPE-2 FUZZY LOGIC SYSTEMS

4.1 Introduction

In this chapter, we discuss one of the parameters for QoS: packet transmission delay. And our algorithm is quite different from all the previous works. We proposed to use interval type-2 FLS for packet transmission delay analysis and prediction, and we compared it against a singleton type-1 FLS.

We applied the transmission delay predictors to control the transmission power. The simulation achieved performance parameters of average delay, energy consumption and throughput. Assume we knew the actual transmission delay, we also got these parameters as the performance bounds.

4.2 Preliminaries

4.2.1 Bit Error Rate

BER is the percentage of bits with errors divided by the total number of bits that have been transmitted, received or processed over a given time period. It is a measure of transmission quality. The high BER means high packets loss ratio. Requests for resends will increase delay. For delay sensitive traffic requires a very low BER.

4.2.2 MAC Layer Service Time

There are three basic processes when the MAC layer transmits a packet [43]: the decrement process of the backoff timer, the successful packet transmission process that takes a time period of T_{suc} and the packet collision process that takes a time period of T_{col} . Here, T_{suc} is the random variable representing the period that the medium is sensed

busy because of a successful transmission, and T_{col} is the random variable representing the period that the medium is sensed busy by each station due to collisions. The MAC layer service time is the time interval from the time instant that a packet becomes the head of the queue and starts to contend for transmission, to the time instant that either the packet is acknowledged for a successful transmission or the packet is dropped. This time is important when we examine the performance of higher protocol layers.

4.2.3 Packet Transmission Delay

The packet delay represents the time it took to send the packet between the transmitter and the next-hop receiver, including the deferred time and the time to fully acknowledge the packet. The packet transmission delay between the mobile nodes includes three parts: the wireless channel transmission delay, the Physical/MAC layer transmission delay, and the queuing delay [18].

Defining D as the distance between two nodes and C as the light speed, the wireless channel transmission delay as:

$$Delay_{ch} = \frac{D}{C} \quad (4.1)$$

The Physical/MAC layer transmission delay will be decided by interaction of the transmitter and the receive channel, the node density and the node traffic intensity etc. The queuing delay is decided by the mobile node I/O system-processing rate, the subqueue length in the node. In order to make the system “stable”, the rate at which node transfers packets intended for its destination must satisfy all nodes that the queuing lengths will not be infinite and the average delays will be bounded.

4.3 Overview of Interval Type-2 Fuzzy Logic Systems

Figure 4.1 shows the structure of a type-2 FLS [44]. It is very similar to the structure of a type-1 FLS [45]. For a type-1 FLS, the *output processing* block only

contains the defuzzifier. We assume that the reader is familiar with type-1 FLSs, so that here we focus only on the similarities and differences between the two FLSs.

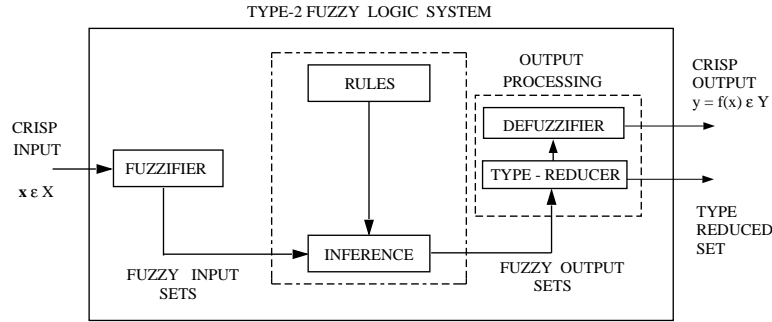


Figure 4.1. The structure of a type-2 FLS.

In order to emphasize the importance of the type-reduced set, we have shown two outputs for the type-2 FLS, the type-reduced set and the crisp defuzzified value.

The fuzzifier maps the crisp input into a fuzzy set. This fuzzy set can, in general, be a type-2 set.

In the type-1 case, we generally have “IF-THEN” rules, where the l th rule has the form “ R^l : IF x_1 is F_1^l and x_2 is F_2^l and \dots and x_p is F_p^l , THEN y is G^l ”, where: x_i s are inputs; F_i^l s are antecedent sets ($i = 1, \dots, p$); y is the output; and G^l s are consequent sets. The distinction between type-1 and type-2 is associated with the nature of the membership functions, which is not important while forming rules; hence, the structure of the rules remains exactly the same in the type-2 case, the only difference being that now some or all of the sets involved are of type-2; so, the l th rule in a type-2 FLS has the form “ R^l : IF x_1 is \tilde{F}_1^l and x_2 is \tilde{F}_2^l and \dots and x_p is \tilde{F}_p^l , THEN y is \tilde{G}^l ”.

In the type-2 case, the inference process is very similar to that in type-1. The inference engine combines rules and gives a mapping from input type-2 fuzzy sets to

output type-2 fuzzy sets. To do this, one needs to find unions and intersections of type-2 sets, as well as compositions of type-2 relations.

In a type-1 FLS, the defuzzifier produces a crisp output from the fuzzy set that is the output of the inference engine, i.e., a type-0 (crisp) output is obtained from a type-1 set. In the type-2 case, the output of the inference engine is a type-2 set; so, “extended versions” (using Zadeh’s Extension Principle [46]) of type-1 defuzzification methods was developed in [44]. This extended defuzzification gives a type-1 fuzzy set. Since this operation takes us from the type-2 output sets of the FLS to a type-1 set, this operation was called “type-reduction” and the type-reduced set so obtained was called a “type-reduced set” [44]. To obtain a crisp output from a type-2 FLS, we can defuzzify the type-reduced set.

General type-2 FLSs are computationally intensive, because type-reduction is very intensive. Things simplify a lot when secondary membership functions (MFs) are interval sets (in this case, the secondary memberships are either 0 or 1). When the secondary MFs are interval sets, the type-2 FLSs were called “interval type-2 FLSs”. In [47], Liang and Mendel proposed the theory and design of interval type-2 fuzzy logic systems (FLSs). They proposed an efficient and simplified method to compute the input and antecedent operations for interval type-2 FLSs, one that is based on a general inference formula for them. They introduced the concept of upper and lower membership functions (MFs) and illustrate their efficient inference method for the case of Gaussian primary MFs. They also proposed a method for designing an interval type-2 FLS in which they tuned its parameters.

In an interval type-2 FLS with *singleton fuzzification* and meet under minimum or product t -norm, the result of the input and antecedent operations, F^l , is an interval type-1 set, i.e., $F^l = [\underline{f}^l, \overline{f}^l]$, where \underline{f}^l and \overline{f}^l simplify to

$$\underline{f}^l = \underline{\mu}_{\tilde{F}_1^l}(x_1) \star \dots \star \underline{\mu}_{\tilde{F}_p^l}(x_p) \quad (4.2)$$

and

$$\overline{f}^l = \overline{\mu}_{\tilde{F}_1^l}(x_1) \star \dots \star \overline{\mu}_{\tilde{F}_p^l}(x_p) \quad (4.3)$$

where x_i ($i = 1, \dots, p$) denotes the location of the singleton.

In this chapter, we use center-of-sets type-reduction, which can be expressed as:

$$Y_{\text{cos}}(Y^1, \dots, Y^M, F^1, \dots, F^M) = [y_l, y_r] = \int_{y^1} \dots \int_{y^M} \int_{f^1} \dots \int_{f^M} 1 / \frac{\sum_{i=1}^M f^i y^i}{\sum_{i=1}^M f^i} \quad (4.4)$$

where Y_{cos} is an interval set determined by two end points, y_l and y_r [47]; $f^i \in F^i = [\underline{f}^i, \overline{f}^i]$; $y^i \in Y^i = [y_l^i, y_r^i]$, and Y^i is the centroid of the type-2 interval consequent set \tilde{G}^i ; and, $i = 1, \dots, M$. Because Y_{cos} is an interval set, we defuzzify it using the average of y_l and y_r ; hence, the defuzzified output of an interval type-2 FLS is

$$f(\mathbf{x}) = \frac{y_l + y_r}{2} \quad (4.5)$$

4.4 Modeling BER and MAC Layer Service Time Using Interval Type-2 Membership Function

4.4.1 BER Analysis and Modeling BER

Let p be the probability that bit is error in any given time. So p can be described as a random variable with a known mean value E_a .

Now, at any given time the bit is error with probability p and the bit is correct with probability $1-p$. Since the bit is either error or correct, the number of the bits it is error (E_b) for a fixed length transmission bits is binomial random variable. The length of the transmission bits is N_t , The probability that E_b takes any value x is :

$$P\{E_b = x\} = C_x^{N_t} p^x (1-p)^{N_t-x} \quad (4.6)$$

As the number of the length of the transmission bits increase, the binomial distribution is approximated to a Gaussian distribution, with mean $\mu = pN_t$ and variance $\sigma^2 = p(1-p)N_t$.

In this chapter, we set up membership functions (MFs) for BER. We get the original data from 10000 Monte-Carlo simulations. From the original data of BER shown in Table 4.1, we randomly decomposed the whole data sets into ten segments and computed the mean m_i and std σ_i of the BER of the i th segment, $i = 1, 2, \dots, 10$. We also computed the mean m and std σ of the entire BER. To see which value $-m_i$ or σ_i varies more, we normalized the mean and std of each segment using m_i/m , and σ_i/σ , and we then computed the std of their normalized values, σ_m and σ_{std} .

Table 4.1. Mean and std values for ten segments and the entire BER, and their normalized std.

| BER | mean | std |
|----------------|----------|----------|
| Segment 1 | 0.016613 | 0.033315 |
| Segment 2 | 0.015618 | 0.027857 |
| Segment 3 | 0.015528 | 0.017401 |
| Segment 4 | 0.016206 | 0.02107 |
| Segment 5 | 0.015721 | 0.017148 |
| Segment 6 | 0.016298 | 0.029309 |
| Segment 7 | 0.017062 | 0.037428 |
| Segment 8 | 0.016253 | 0.022871 |
| Segment 9 | 0.016448 | 0.023194 |
| Segment 10 | 0.016237 | 0.020675 |
| Entire Traffic | 0.016198 | 0.025829 |
| Normalized std | 0.029161 | 0.26184 |

As we see from the last row of Tables 4.1, $\sigma_m \ll \sigma_{std}$. We conclude, therefore, that if the BER of each segment (small number of simulations) are Gaussian, then the

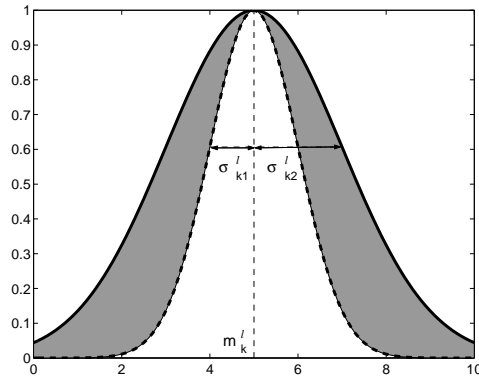


Figure 4.2. Type-2 Gaussian MF with uncertain standard deviation.

membership function for BER (in large number of simulations) is more appropriate to be modeled as Gaussian with uncertain standard deviation. One example of type-2 Gaussian MF with uncertain standard deviation is shown in Fig.4.2.

4.4.2 MAC Layer Service Time Analysis and Modeling

Recent research by Zhai, kwon and Fang [43] discovered that the lognormal distribution could match for the MAC layer service time. i.e., if the MAC layer service time for the packet i is s_i , then

$$\log_{10} s_i \sim \mathcal{N}(\cdot; m, \sigma^2) \quad (4.7)$$

We, therefore, tried to model the logarithm of the MAC layer service time, to see if a Gaussian MF can match its nature. We got the original data from simulation. We decomposed the whole data sets into ten segments and computed the mean m_i and std σ_i of the logarithm of the MAC layer service time of the i th segment, $i = 1, 2, \dots, 10$. We also computed the mean m and std σ of the entire logarithm of the MAC layer service time. To see which value $-m_i$ or σ_i varies more, we normalized the mean and std of each segment using m_i/m , and σ_i/σ , and we then computed the std of their normalized values, σ_m and σ_{std} .

Table 4.2. Mean and std values for ten segments and the entire logarithm of MAC layer service time, and their normalized std.

| MAC layer service time | mean | std |
|------------------------|-----------|----------|
| Segment 1 | -1.1902 | 0.44295 |
| Segment 2 | -1.1929 | 0.44698 |
| Segment 3 | -1.1967 | 0.45237 |
| Segment 4 | -1.1959 | 0.44835 |
| Segment 5 | -1.1917 | 0.43598 |
| Segment 6 | -1.1924 | 0.44779 |
| Segment 7 | -1.1976 | 0.45687 |
| Segment 8 | -1.1996 | 0.45554 |
| Segment 9 | -1.1923 | 0.45068 |
| Segment 10 | -1.1997 | 0.462 |
| Entire Traffic | -1.1949 | 0.44981 |
| Normalized std | 0.0028746 | 0.016421 |

As we see from the last row of Tables 4.2, $\sigma_m \ll \sigma_{std}$. We conclude, therefore, that if the logarithm of the MAC layer service time of each segment (small number of simulations) are Gaussian, then the membership function for the logarithm of the MAC layer service time (in large number of simulations) is more appropriate to be modeled as Gaussian with uncertain standard deviation. One example of type-2 Gaussian MF with uncertain standard deviation is shown in Fig.4.2.

4.5 Cross-Layer Design Using Interval Type-2 Fuzzy Logic System

As we introduce in the Section 2, the high BER means high packets loss rate. Requests for resends will increase latency. For delay sensitive traffic requires a very low BER. And the MAC layer service time is important when we examine the performance of higher protocol layers. So we could know BER and MAC layer service time will manage the packet transmission delay between the mobile nodes. We are now ready to evaluate the packet transmission delay using fuzzy logic systems.

We predicted packet transmission delay based on the following two antecedents:

1. Antecedent 1. BER.
2. Antecedent 2. MAC layer service time.

The consequent was depicted as the packet transmission delay. The linguistic variables used to represent the BER and MAC layer service time were divided into three levels: *low*, *moderate*, and *high*. The consequent – the packet transmission delay was divided into 5 levels, *very low*, *low*, *moderate*, *high* and *very high*.

We designed questions such as:

IF *BER* is *low* and *MAC layer service time* is *high*, THEN the packet transmission delay is _____.

So we need to set up $3^2 = 9$ (because every antecedent has 3 fuzzy sub-sets, and there are 2 antecedents) rules for this FLS. We summarized these rules in Table 4.3.

Table 4.3. Fuzzy Rules and Consequent

| <i>Antecedent1</i> | <i>Antecedent2</i> | <i>Consequent</i> |
|--------------------|--------------------|-------------------|
| <i>Low</i> | <i>Low</i> | <i>VeryLow</i> |
| <i>Low</i> | <i>Moderate</i> | <i>Low</i> |
| <i>Low</i> | <i>High</i> | <i>Moderate</i> |
| <i>Moderate</i> | <i>Low</i> | <i>Low</i> |
| <i>Moderate</i> | <i>Moderate</i> | <i>Moderate</i> |
| <i>Moderate</i> | <i>High</i> | <i>High</i> |
| <i>High</i> | <i>Low</i> | <i>Moderate</i> |
| <i>High</i> | <i>Moderate</i> | <i>High</i> |
| <i>High</i> | <i>High</i> | <i>VeryHigh</i> |

We used Gaussian membership functions (MFs) to represent the antecedents and the consequent.

Fig.4.3 show the FLS application for the cross-layer design.

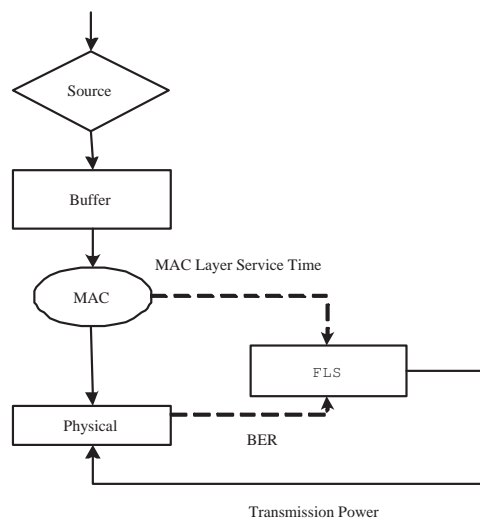


Figure 4.3. FLS application for cross-layer design.

When a mobile node sends out a packet, it will first predict the packet transmission delay using the FLS algorithm. After that, the node could adjust the transmission power according to the predicted packet transmission delay. That means if the predicted packet transmission delay is large, we will increase the transmission power. Similar rules can be obtained for other cases. Therefore average delay, energy consumption and throughput performances will change.

4.6 Simulations

We implemented the simulation model using the OPNET modeler. The simulation region was 300×300 meters. There were 12 mobile nodes in the simulation model, and the nodes were roaming independently with variable ground speed between 0 to 10 meters per second. The mobility model was called one-step Markov path model. The movement would change the distance between mobile nodes. We assumed the collecting data distribution of the mobile node was exponential distribution and the arriving interval was 0.2 second and the length of the packet is 512 bits.

For type-1 FLS, We chose Gaussian membership function as antecedents; for interval type-2 FLS, we used Gaussian primary MF's with fixed mean and uncertain std for the antecedents. The initial 9 rules were designed according to Table 4.3. We followed the training algorithm proposed in [47]. In [48], the Back-prop NN is the best non-fuzzy design. We chose Back-prop NN as a comparison. We set the Back-prop NN as two input, one output, 4 layers and 540 connectivity. The steepest decent algorithm was used to train all the parameters based on the 300 data sets. After training, the rules were fixed, and we tested the FLS based on the remaining 300 data sets.

In Fig.4.4, we summarized the root-mean-square-errors (RMSE) between the estimated packet transmission delay and the actual delay.

$$RMSE = \sqrt{\frac{1}{300} \sum_{i=301}^{600} [d(i) - f(i)]^2} \quad (4.8)$$

where $d(i)$ was the actual packet transmission delay and $f(i)$ was the estimated delay.

The simulation result shows that the interval type-2 FLS for packet transmission delay analysis and prediction outperforms the type-1 FLS, and two FLSs outperform Back-prop NN.

In the following performance simulation, we assumed we could know the actual transmission delay. We used it as a ideal case to get the performance parameters as the bounds.

4.6.1 Average Delay

We used the average delay parameter to evaluate the network performance. Each packet was labeled a timestamp when it was generated by the source sensor node. When its destination sensor node received it, the time interval was the transmission delay.

$$Average\ Delay = \frac{\sum_{i=1}^K D_i}{K} \quad (4.9)$$

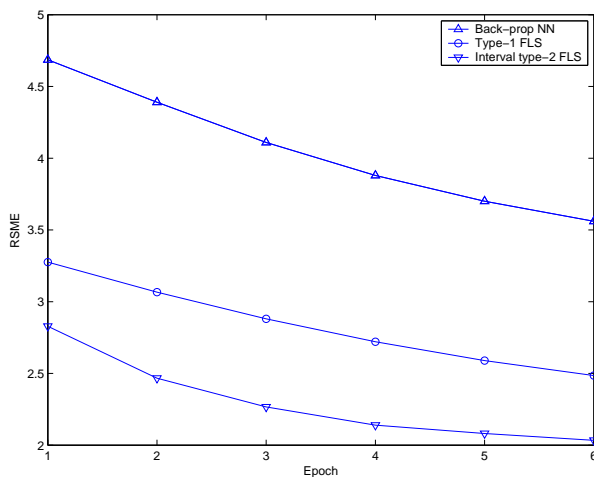


Figure 4.4. The RMSE of packet transmission delay prediction for two FLS approaches.

Fig.4.5 summarized the delay performance of the four algorithms. The type-2 FLS algorithm was better than the type-1 FLS algorithm. The type-2 FLS predictor could reduce the average delay by up to 20% than type-1 FLS predictor. Two FLS were better than Back-prop NN algorithm. And the ideal case was get by using actual transmission delay as the predictor outcome, and it was the best performance among the four.

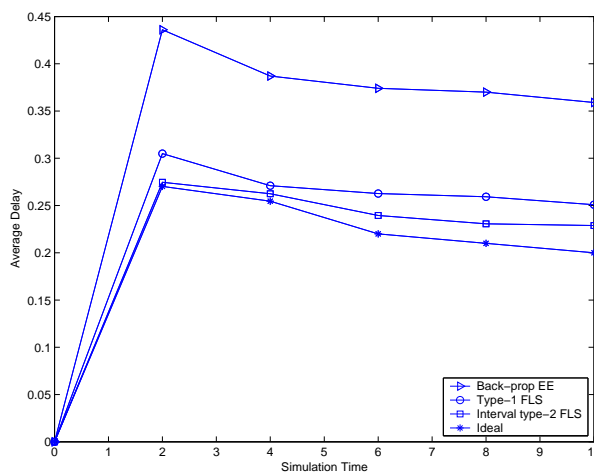


Figure 4.5. Average Delay for Three Algorithms.

4.6.2 Energy Efficiency

It is not convenient to recharge the battery, so the energy efficiency was extremely important for mobile ad hoc networks. In the wireless mobile ad hoc networks, we used the parameter: the remaining energy to describe the energy efficiency.

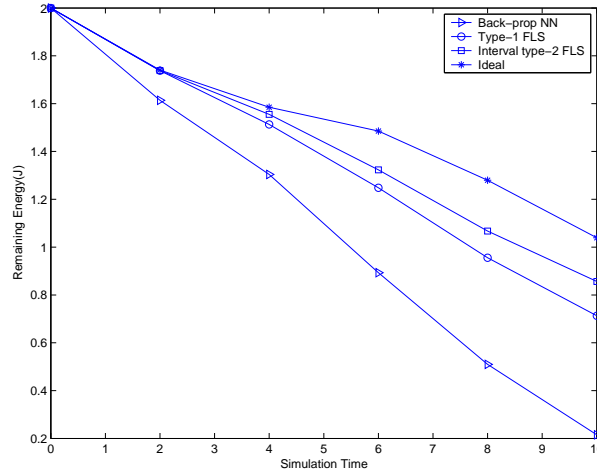


Figure 4.6. Remaining Energy for Three Algorithms.

The fuzzy computing consumed energy. In [42], we knew the energy consumed by computing was far less than that consumed by communication. We could only consider the communication energy consumption for energy efficiency.

Fig.4.6 showed the remaining energy of the four algorithms. We assumed that the energy of each sensor is 2.0J and we adopted CSMA/CA protocol to solve the packets collision problem. If a sensor node transmitted N_s packets (each packet cost 1 second) and receives N_r packets (each packets also cost 1 second) and it was roaming in the network for T_m , we could get the remaining energy E_i of this sensor node [18]:

$$E_i = 2.0 - (3 \times 10^{-5} \times T_m + 1.2 \times 10^{-3} \times N_s + 6 \times 10^{-4} \times N_r) \quad (4.10)$$

Same as the average delay, for the performance of the energy consumption, the type-2 FLS algorithm was better than the type-1 FLS algorithm. The type-2 FLS predictor could reduce the energy consumption by up to 21% than the type-1 FLS predictor. Two FLSs were better than Back-prop NN algorithm. The ideal case was set as the low bound.

4.6.3 Networks Efficiency

The mobile ad hoc networks are used to collect data and transfer packets. The throughput of packets transmitted is one of the parameters to evaluate the networks efficiency. In our simulation, we assumed the collecting data distribution of the mobile node was Poisson distribution and the arriving interval was 0.2 second.

Observing from Fig.4.7, the type-2 FLS algorithm was better than the type-1 FLS algorithm. The type-2 FLS predictor could increase the throughput by up to 45% than the typ-1 FLS predictor. Two FLSs were better than Back-prop NN algorithm. And the ideal case was set as the high bound.

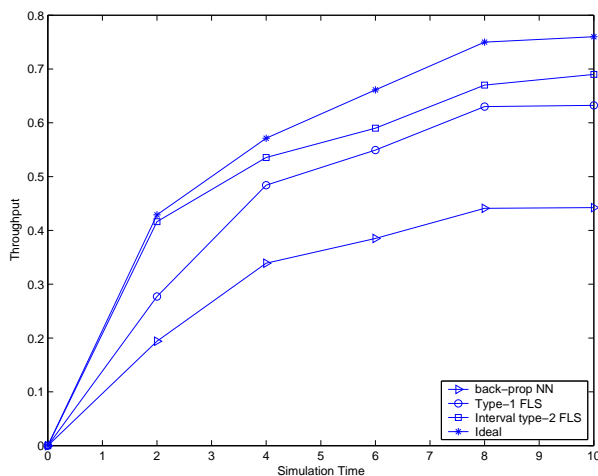


Figure 4.7. Throughput for Three Algorithms.

We introduced the fuzzy logic system in the cross-layer design. Compared with other algorithms for cross-layer design, the fuzzy method could be flexible and simpler to implement. We could predict the packet transmission delay according to the information just from physical layer and MAC layer. So we have potential application advantage. We use the FLSs as the predictors and we could control the transmission power according the outcomes of the predictors. Simulation results showed that the type-2 FLS algorithm is better than the type-1 FLS algorithm. Two FLSs were better than Back-prop NN algorithm. And we could set the ideal case as the performance bounds.

4.7 Conclusion

Cross-layer design is a effective method to improve the performance of the mobile ad hoc network. We applied the fuzzy logic system to coordinate the physical layer and the data-link layer. We selected BER and MAC layer service time as antecedents to analyze and predict the packet transmission delay. And we applied a type-1 FLS and an interval type-2 FLS for the packet transmission delay analysis and prediction. Simulation results showed that the interval type-2 FLS for packet transmission delay analysis and prediction outperforms the type-1 FLS. Two FLSs are better than Back-prop NN algorithm. We used the FLSs as the predictors and we could control the transmission power according the outcomes of the predictors. Simulation results showed that the type-2 algorithm is better than the type-1 algorithm. Two FLSs are better than Back-prop NN algorithm. And we could set the ideal case as the performance bounds.

CHAPTER 5

CROSS-LAYER DESIGN FOR IMAGE TRANSMISSION IN WIRELESS SENSOR NETWORKS

5.1 Introduction

Image is one of the major traffic in Wireless sensor networks. However, existing wireless sensor networks provide only limited quality of service (QoS) for image application. Hence, We could consider cross-layer design for image transmission in wireless sensor networks. We combine the application layer, the MAC layer and the physical layer together. According to analysis and simulation, high priority service will achieve better PSTR performance. Low priority service could achieve better average delay performance at the beginning, and it will become worse later. There are tradeoffs between QoS and energy consumption for both high priority service and low priority service. Application level Qos was applied to evaluate the cross-layer design for WSNs [51].

5.2 Overview of Cross-layer Design

In our cross-layer design, we considered three layers: the application layer, the MAC layer and the physical layer. Fig.5.1 shows the structure of this design.

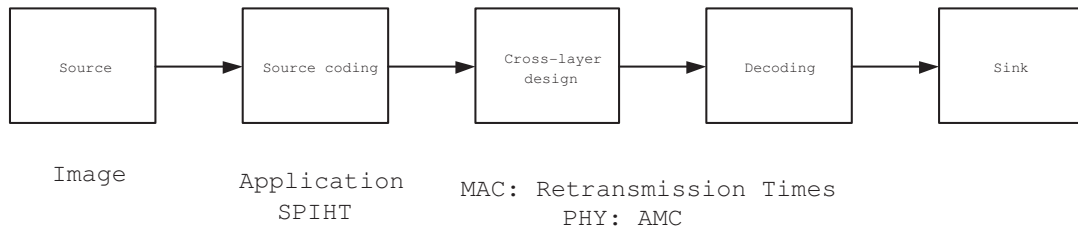


Figure 5.1. Structure of Cross-layer Design.

As we know, SPIHT codes the most important wavelet transform coefficients in priority, and put them in the front of the coded data. We could apply service differential in application layer. We divide the data into two priorities and the service differentiation aims at improving the service of high-priority classes. We set the first part of data as high priority and the remaining data as low priority.

For the MAC layer, the maximum retransmission times will manage the frame loss ratio and the energy consumption. We set large number for high priority service and small number for low priority service. Large retransmission times will decrease frame loss ratio. However, small retransmission times will decrease delay and energy consumption.

In the 802.11A physical protocol, eight AMC modes are used in physical layer. We set small mode number for high priority service. This is also a kind of tradeoff for QoS parameters. The smaller the mode number, the better BER performance, and the larger delay. On the contrast, the larger the mode number, the higher speed, the less energy consumption to overcome interference and noise.

5.3 Simulation and Analysis

We implemented the SPIHT using Matlab, and implemented communication system using the OPNET modeler. The simulation region was 300×300 meters. There were 9 mobile nodes in the simulation model, and the nodes were roaming independently with variable ground speed between 1 to 10 meters per second. The mobility model was called one-step Markov path model. The movement would change the distance between mobile nodes.

Table 5.1 showed simulation parameters that were used in application layer. The compressed image had 26199 bits data. We divided all the image data into high priority data and lower priority data. We could see there was service differential in case 1 and

case 4. In case 2 and case 3, we applied cross-layer design and we divided the data into different portion for high priority service and low priority service.

Table 5.1. Design Cases

| <i>Design</i> | <i>HighPriority</i> | <i>LowPriority</i> | <i>Total</i> |
|---------------|---------------------|--------------------|--------------|
| 1 | 26199 | 0 | 26199 |
| 2 | 20000 | 6199 | 26199 |
| 3 | 4000 | 22199 | 26199 |
| 4 | 0 | 26199 | 26199 |

Table 5.2 showed simulation parameters settings in the MAC layer, the physical layer and energy consumption. Retransmission times are the maximum retransmission times in MAC layer.

Table 5.2. Parameters Setting

| | <i>MACRetransmissionTimes</i> | <i>AMC</i> | <i>Power</i> |
|---------------------|-------------------------------|------------|--------------|
| <i>HighPriority</i> | 8 | 1 | 0.20 |
| <i>LowPriority</i> | 3 | 8 | 0.10 |

5.3.1 Packet Successful Transmission Ratio

Because we increased the maximum retransmission time and transmitted power to overcome noise and interference, we could achieve better performance in packet successful transmission ratio for high priority. Simulation result in Fig.5.2 showed high priority design could have better Packet Successful Transmission Ratio (PSTR) performance. Fig.5.2 also showed if we selected large portion of data as high priority, we could achieve

better PSTR performance. Comparing design 2 with 3, the PSTR performance in design 2 was up to 25.4% larger.

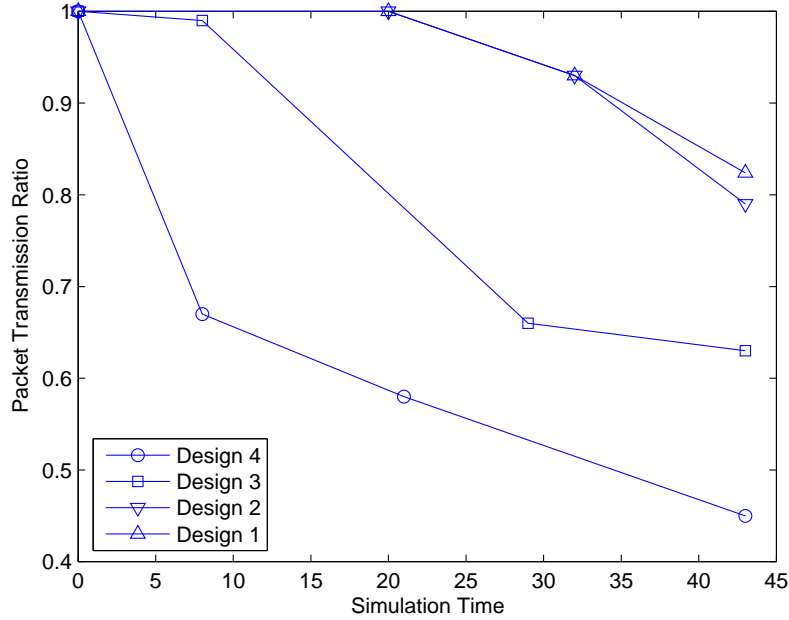


Figure 5.2. Packet Successful Transmission Ratio.

5.3.2 Average Delay

We used the average delay to evaluate the delay performance. K was the received packets number.

$$d_{average} = \frac{\sum_{i=1}^k d_i}{k} \quad (5.1)$$

According to analysis, small retransmission times would decrease delay. Fig.5.3 showed the delay performance of the high priority was worse than that of low priority at the beginning. However the delay performance of high priority would be better than that of low priority later. This was because low priority had low PSTR, and a large number of packets were dropped duo to low PSTR. As showed in Fig.5.3., we concluded that design

2 achieve the best delay performance, which meant the portion of high priority data was large than that of low priority data could achieve the best delay performance.

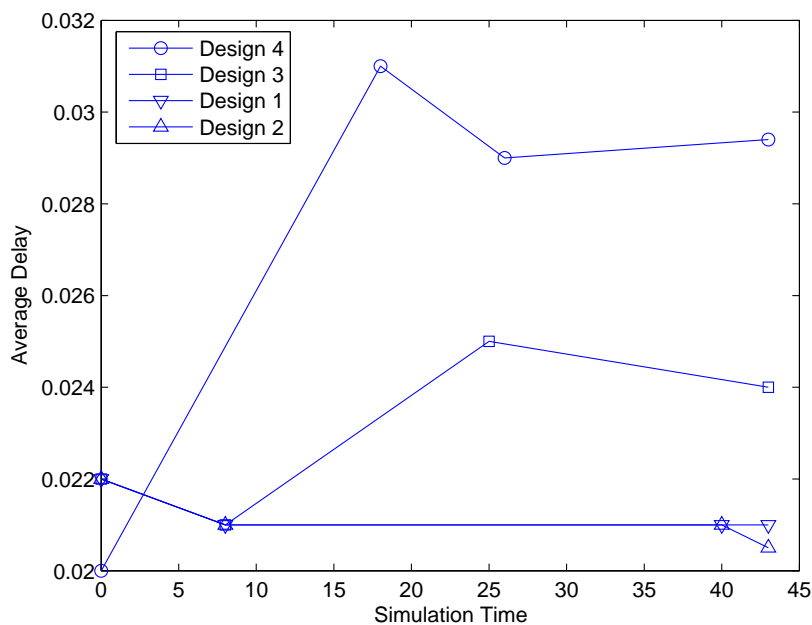


Figure 5.3. Average Delay.

5.3.3 Energy Efficiency

It is not convenient to recharge the battery, so the energy efficiency is extremely important for wireless sensor networks. High priority service would cost more energy than low priority service. Low priority service would cost less energy because it was less important according to SPIHT image compressed algorithm. Simulation result in Fig.5.4 matched our analysis. There was a tradeoff between the QoS performance and the energy efficiency.

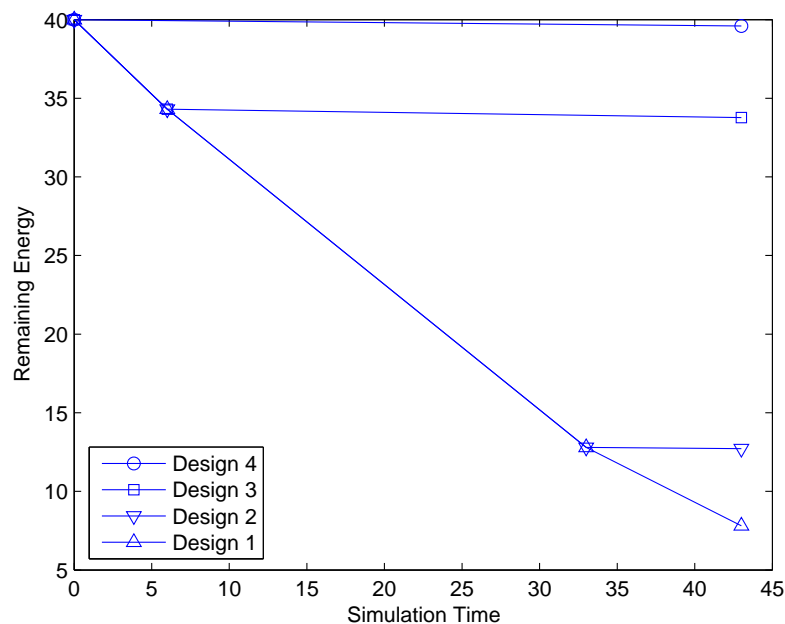


Figure 5.4. Remaining Energy.

5.3.4 Image Quality

PSTR could only indicate packet level QoS. Application level QoS was more important in case of image transmission. We use 0.1 as the SPIHT compressed ratio. According to our analysis, we knew that high priority service would achieve better QoS quality for both application level and packet level. The simulation result was same as our analysis. We listed the PSNR(Peak signal-to-noise ratio)and SSIM (Structural SIMilarity)index for four designs in table 5.3. We could conclude that the application QoS was exactly a tradeoff with the energy consumption.

Fig.5.5 showed the images for four designs. Design 4 had the worst application level QoS performance, but it consumed the least energy.

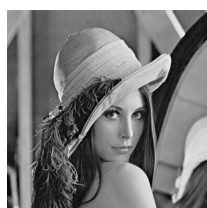
We introduced the cross-layer design for image transmission in WSNs. Comparing the performance of QoS and energy efficiency, the cross-layer design could be flexible and simpler to implement and the performance outputs were also impressive.

Table 5.3. Image Quality

| <i>Design</i> | <i>PSNR</i> | <i>SSIM</i> |
|---------------|-------------|-------------|
| 1 | 29.31 | 0.8027 |
| 2 | 27.75 | 0.7683 |
| 3 | 23.08 | 0.6007 |
| 4 | 19.59 | 0.4699 |

5.4 Conclusion

Cross-layer design is an effective approach for image transmission in WSNs. In this chapter, we introduce the cross-layer design for the application layer, the MAC layer and the physical layer. Analysis and simulation results showed the cross-layer design could benefit image transmission in wireless sensor networks. High priority service would achieve better PSTR performance. Low priority service achieved better delay performance at the beginning, and it became worse later. For high priority service, it would cost more energy than low priority service. Application level QoS was applied to evaluate the cross-layer design for WSNs.



Original Image



Compressed Image



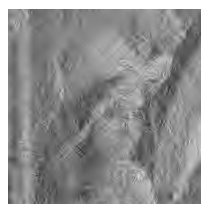
Design 1



Design 2



Design 3



Design 4

Figure 5.5. The Image Results.

CHAPTER 6

LATENCY-AWARE AND ENERGY EFFICIENCY TRADEOFFS FOR WIRELESS SENSOR NETWORKS

6.1 Introduction

WSNs are likely to be widely deployed in commercial and military applications. However, several obstacles need to be overcome, such as latency-aware and energy efficiency [53] [17]. Latency-aware means to transfer the packets among sensors as quickly as possible. Energy efficiency means to the networks should function for as long as possible [58].

The cell-partitioned model is adopted in this chapter (Fig.6.1). We can assume that the network is divided into non-overlapping cells, each cell is of equal size [54].

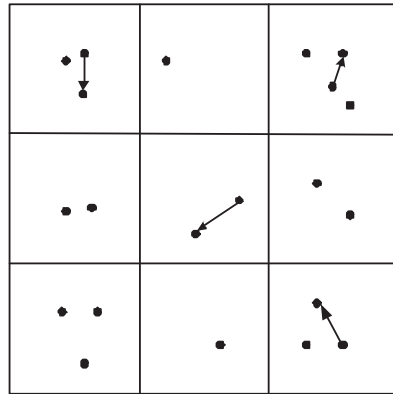


Figure 6.1. A Cell-partitioning Wireless Sensor Network.

The sensor nodes are roaming independently from one cell to another. If two sensor nodes are in the same cell, they can transfer packets with each other, and sensor nodes within different cells cannot communicate with each other. The sensor nodes have a variable mobility speed and the actual mobility can be described by one-step Markov

path model [21]. Each sensor node can generate packets with a Poisson distribution and each sensor node can reserve original and relay packets. Each packet enters its subqueue according to its destination node ID. This model can simplify the scheduling complexity and facilitates analysis. It can also conceal the detail of global network topology from the individual sensor node [55].

In this chapter, we consider the tradeoffs between the delay performance and the energy efficiency offered by the cell partitioned wireless model. The contributions are twofold: First, we classified the sensor service into two priorities: high and low. The higher priority, the better delay performance and more energy consumption. We realized it with the two-hop relay algorithm, and we establish energy/delay tradeoffs curve for the performance of the two-hop relay algorithm. Second, The FLS is used to elect the three relay nodes. When there are several pairs within one cell, we use the FLS to elect the destination node.

Generally, a node with the maximum remaining energy capacity or a node with the nearest distance to the source node or a node with the highest degree of mobility is elected as the relay/destination node.

The remainder of this chapter is structured as following. In Section 6.2, we introduced the energy, delay, and the two-hop relay algorithm. In Section 6.3, we applied the FLS into the two-hop relay algorithm. Simulation results and discussions were presented in Section 6.4. In Section 6.5, we concluded the chapter.

In this chapter, we designed a FLS for relay/destination nodes election. The rules were designed to be based on the knowledge from a group of network experts.

6.2 Energy And The 2-Hop Relay Algorithm

6.2.1 Energy

A sensor node consumes significant power when it either transmits a packet or when it receives a packet. It will also consume energy when the sensor node is idle because the sensor node keeps moving. The energy consumption ratio of Transmit: Receive: Idle is approximately 40:20:1 [56].

6.2.2 The Two-hop Relay Algorithm

This relay algorithm restricts packets to 2-hop paths, and the relay packet is inserted into the subqueue of the relay sensors until a source encounters its destination.

We summarize the two-hop relay algorithm as follows [57]:

1) If there exists source-destination pairs within a cell, there are two options:

- If there exists one source-destination pair within a cell and if the source contains a new packet intended for that destination, transmit.
- If there exists more than one source-destination pair within a cell, choose the sensor with the longest subqueue as the source and choose the sensor with the energy most as the destination and transmit it.

2) If there is no source-destination pair in a cell, there are two options:

- Send a relay packet to its destination: if the designated transmitter has a packet destined for the designated receiver, send the packets to the receiver.
- Send a new relay packet:
 1. For high priority sensor: if the designated transmitter has a new packet that has never before been transmitted, conserve the packet in its own subqueue according to its destination. Choose the three energy most sensors as the relay destinations and transmit three copies to them.

2. For low priority sensor: conserve the packet in its own subqueue according to its destination.

This algorithm restricts all routes to 2-hop while the relay packets are only allowed to transmit to their destinations. We pick up the packet reserved in the subqueue with the longest queuing length to keep the queuing length in balance among the sensors in order to reduce the time jitter. We chose the sensors with most energy as the destination to keep the energy in balance among sensors.

6.2.3 Cell Location Algorithm

Each sensor node knows its location (X position, Y position). As all the cells are of equal size, each sensor node can determine the cell serial number it belongs to.

For example, the network size is $N \times N$ and it is partitioned into $C = S^2$ cells:

$$C_{sn} = \left[\frac{X \cdot S}{N} \right] + \left[\frac{Y \cdot S}{N} \right] \cdot S + 1 \quad (6.1)$$

Where $[]$ refers to the round function and it will round the value of the float argument to the nearest integer value.

Every sensor node will send a “Hello” message with its cell serial number C_{sn} and other information to other sensor nodes between a constant time interval. When a sensor node with ID number A receives a “Hello” message sent by sensor node B, sensor node A compares its cell serial number C_{sna} with the cell serial number C_{snb} of sensor node B.

- If C_{sna} is equal to C_{snb} , which means sensor node A and sensor node B are in the same cell and if the information of sensor node B is already in the database of sensor node A, update the information of sensor node B.
- If C_{sna} is equal to C_{snb} , which means sensor node A and sensor node B are in the same cell and if the information of sensor node B is not in the database of sensor node A, record the information of sensor node B.

- If C_{sna} is not equal to C_{snb} , which means sensor node A and sensor node B are not in the same cell and if the information of sensor node B is in the database of sensor node A, delete the information of sensor node B.
- If C_{sna} is not equal to C_{snb} , which means sensor node A and sensor node B are not in the same cell and if the information of sensor node B is not in the database of sensor node A, remain idle.

Notice that a sensor node only keeps the information of the sensor nodes that in the same cell and keeps updating it. The sensor node can reduce the memory usage and keep the latest information.

6.2.4 In-cell Feedback Algorithm

As there is redundancy in the network, when a packet has been delivered to its destination, its remnant versions of this packet should be ignored by the network. We assume all packets have a sending serials number P_{sn} . P_{sn} combining with the source node ID is unique in the network. When sensor node A receives a packet, it will send out a “notice” message with its sending serials number P_{sn} , source sensor ID B and destination sensor node ID A.

When a sensor node receives the “notice” message, it will search packet in its A subqueue. If there is a packet with sending serials number P_{sn} and source node ID B, remove it from its subqueue. Otherwise, remain idle.

Notice that, no packet will be transmitted to its destination twice. We can reduce the energy consumption and shorten average delay.

6.3 The FLS application for the two-hop relay algorithm

The effect of transmitting redundant packets will consume more energy, however, it will also increase the chance that the nodes which hold the original or relay packets

to reach their destination node. How to elect the relay/destination nodes will determine the energy and latency performance.

We collect the knowledge for node election based on the following three descriptors:

1. distance of a node to the source node,
2. its remaining energy, and
3. its degree of mobility.

The linguistic variables used to represent the distance of a node to the source node were divided into three levels: *near*, *moderate*, and *far*; and those to represent its remaining energy and degree of mobility were divided into three levels: *low*, *moderate*, and *high*. The consequent – the possibility that this node will be elected as a relay/destination nodes – was divided into 5 levels, *Very Strong*, *Strong*, *Medium*, *Weak*, *Very Weak*.

We designed questions such as:

IF *distance of a node to the source node* is *near*, and *its remaining energy* is *low*, and *its degree of mobility* is *moderate*, THEN the possibility that this node will be elected as a relay/destination nodes is _____.

so we need to set up $3^3 = 27$ (because every antecedent has 3 fuzzy sub-sets, and there are 3 antecedents) rules for this FLS.

We created one survey for the network experts. We used rules obtained from the knowledge of 6 network experts. These experts were requested to choose a consequent using one of the five linguistic variables. Different experts gave different answers to the questions in the survey. Table 6.1 summarizes the questions used in this survey, and Table 6.2 captures the results from the completed survey.

We used trapezoidal membership functions (MFs) to represent *near*, *low*, *far*, and *high*, and triangle MFs to represent *moderate*. We show these MFs in Fig.6.2.

In our approach to form a rule base, we chose a single consequent for each rule. To do this, we averaged the centroids of all the responses for each rule and used this average

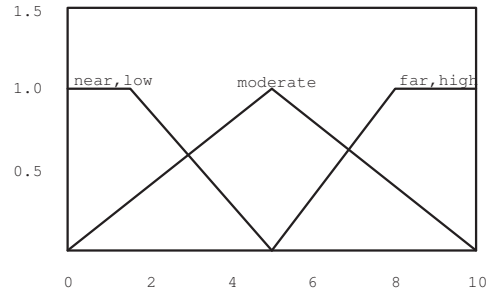


Figure 6.2. MFs for antecedents.

in place of the rule consequent centroid. Doing this leads to rules that have the following form:

R^l : IF *distance of a node to the source node* (x_1) is F_l^1 , and *its remaining energy* (x_2) is F_l^2 , and *its degree of mobility* (x_3) is F_l^3 , THEN the possibility that this node will be elected as a relay/destination node (y) is c_{avg}^l .

where $l = 1, \dots, 27$. c_{avg}^l is defined as

$$c_{avg}^l = \frac{\sum_{i=1}^5 w_i^l c^i}{\sum_{i=1}^5 w_i^l} \quad (6.2)$$

in which w_i^l is the number of people choosing linguistic label i for the consequent of rule l ($i = 1, \dots, 5; l = 1, \dots, 27$) (see Table 6.2); and, c^i is the centroid of the i th consequent set ($i = 1, 2, \dots, 5$). The centroids of the three fuzzy sets depicted in Fig.6.3 are $c^1 = 1.0561$, $c^2 = 3$, $c^3 = 5$, $c^4 = 7$, and $c^5 = 8.9439$.

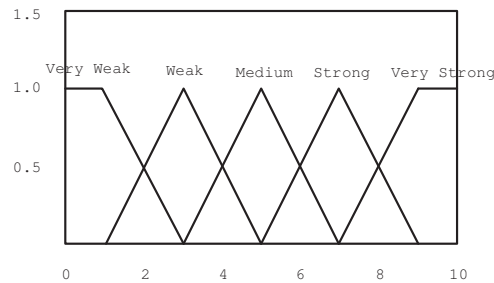


Figure 6.3. MFs for consequent.

To illustrate the use of (6.2), note, for example, that

$$c_{avg}^{11} = \frac{3c^1 + 2c^2 + c^3}{3 + 2 + 1} = 2.3614 \quad (6.3)$$

All 27 c_{avg}^l values are listed in Table 6.2.

For every input (x_1, x_2, x_3) , the output is computed using

$$y(x_1, x_2, x_3) = \frac{\sum_{l=1}^{27} \mu_{F_l^1}(x_1) \mu_{F_l^2}(x_2) \mu_{F_l^3}(x_3) c_{avg}^l}{\sum_{l=1}^{27} \mu_{F_l^1}(x_1) \mu_{F_l^2}(x_2) \mu_{F_l^3}(x_3)} \quad (6.4)$$

6.4 Simulation

We implemented the simulation model using the OPNET modeler. The simulation region is 180×180 meters, and it is divided into 9 non-overlapping cells. Each cell is of equal size, that is 60×60 meters. In the previous section, we know that the energy consumption ratio is 40:20:1. So we can assume that the sensor node consumes approximately 3×10^{-5} watts when idle, 1.2×10^{-3} watts during transmissions and 6×10^{-4} watts during reception.

There were 80 sensor nodes in the simulation model, and the sensor nodes were roaming independently with the ground speed from 1 m/s to 9 m/s. The mobility model is called one-step Markov path model. The probability of moving in the same direction as the previous move is higher than other directions in this model; That means this model has memory.

6.4.1 Average Latency

We use the average latency to evaluate the network performance. It is the average transmission delay of the entire received packet, which is in the same priority. Each packet is labeled a timestamp when it was generated by the source sensor node. When its destination sensor node receives it, the time interval is the transmission delay.

$$Average\ Latency = \frac{\sum_{i=1}^K D_i}{K} \quad (6.5)$$

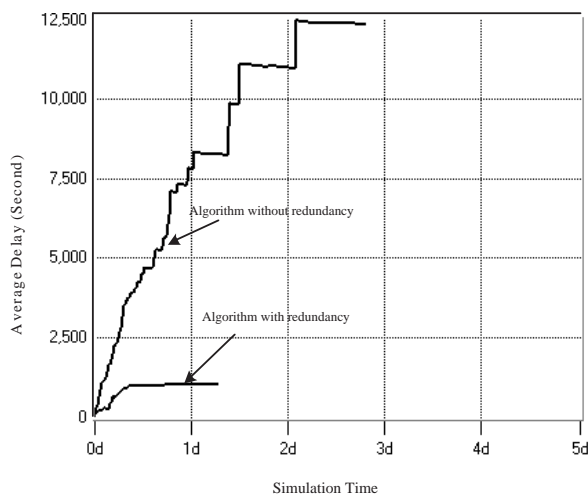


Figure 6.4. Average latency performance of the two algorithms.

Observe Fig.6.4 the latency performance of the algorithm with redundancy for high priority packets is much better than that of the algorithm without redundancy for the low priority packets. Not only the average delay of high priority packets is much smaller than that of the low priority packets, but also the time jitter is much better. Time jitter refers to short-term variation or instability in the duration of a specified time interval. We can draw a conclusion: if the service is time-sensitive, such as video or audio service, we can adopt the scheduling algorithm with redundancy to improve their delay performance.

6.4.2 Energy Efficiency

The algorithm for high priority packets uses the multicast technique to transmit redundant packets to improve the latency performance, however, transmitting redundant packets will consume more energy. The algorithm with redundancy will make its energy efficiency worse than that of the algorithm without redundancy. In the wireless sensor networks, we use two parameters: the number of sensor nodes alive and the remaining energy to describe the energy efficiency.

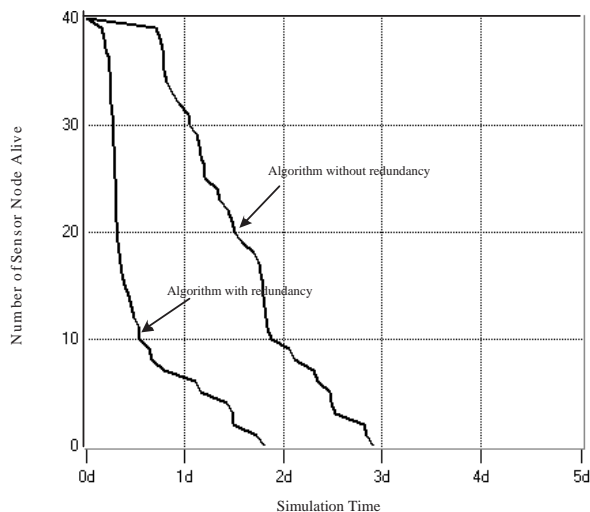


Figure 6.5. Sensor nodes alive of the two algorithms.

When the remaining energy of a sensor node is lower than a certain threshold, the sensor is considered as “dead”. In this simulation, we choose 1.2×10^{-3} as the threshold. This threshold is the minimum energy to transfer a 1K bits packets in a 1K bps bandwidth wireless channel. A sensor is “dead” means it cannot transmit/receive packets any longer, so it will be removed from the sensor network. Sensors are used to collect data and transmit the packets. The number of sensors of wireless sensor networks, which is below a certain threshold, means this network does not work. As Fig.6.5 showed, the remaining sensor nodes alive of the algorithm with redundancy for high priority packets were decreasing much quicker than that of the algorithm without redundancy. As described in the 2-Hop relay algorithm, we chose the sensors with most energy as the destination; we could keep the energy consumption balance among sensors. We could observe from Fig.6.5 that the curve was dropping sharply. Comparing with the average delay performance, we could find it was a tradeoff between network life and delay performance. The simulation result could be a reference when we design the WSNs.

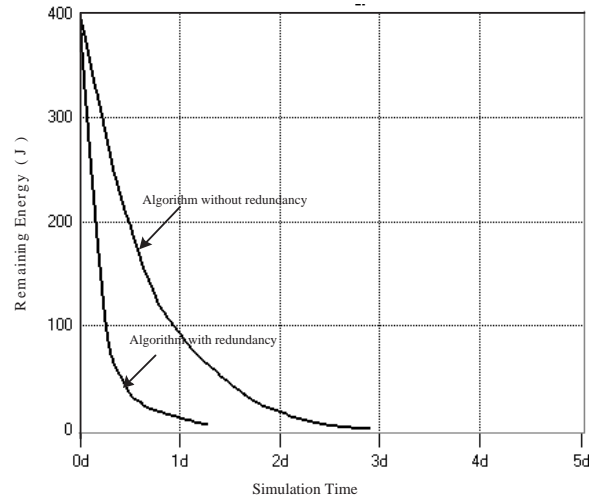


Figure 6.6. Remaining energy of the two algorithms.

Fig.6.6 showed the remaining energy of the two scheduling algorithm. We assumed that the energy of each sensor was 10J and the packet size was 125 bytes (1K bits), and the channel transmission rate is 1K bps. So when the sensor transmitted or received a packet, it would cost 1 second. And we adopt CSMA/CA protocol to solve the packets collision problem. If a sensor node transmitted N_s packets (each packet cost 1 second) and received N_r packets (each packets also cost 1 second) and it was roaming in the network for T_m , we could get the remaining energy E_i of this sensor node:

$$E_i = 10 - (3 \times 10^{-5} \times T_m + 1.2 \times 10^{-3} \times N_s + 6 \times 10^{-4} \times N_r) \quad (6.6)$$

The remaining energy E_w of the whole networks is described as:

$$E_w = \sum_{i=1}^{40} E_i \quad (6.7)$$

Fig.6.6 showed the remaining energy of the algorithm without redundancy is not dropping as sharply as that of the algorithm with redundancy. It illustrated that the algorithm with redundancy cost less energy.

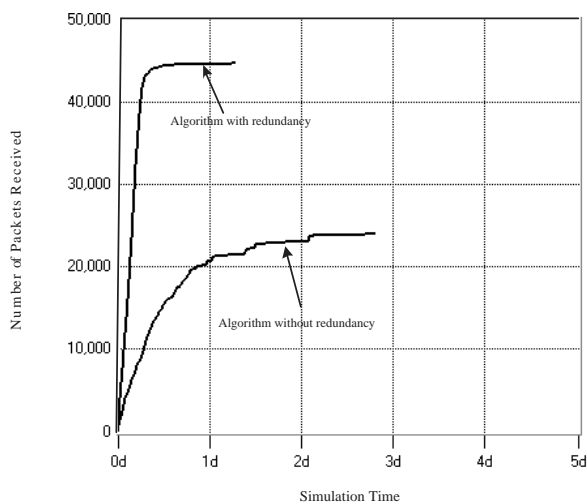


Figure 6.7. Packets received of the two algorithms.

6.4.3 Network quality

The role of the wireless sensor network in the real world is to collect data and transmit packets. In our simulation, we assumed the collecting data distribution of the sensor node is Poisson distribution and the arriving interval was 1 second. Observing from Fig.6.7, although the lifetime of the algorithm with redundancy was shorter than that of the algorithm without redundancy, but it could collect and transmit more packets. One of the main reasons was that the sensors in the networks were keeping moving, that meant it kept consuming energy. For the algorithm without redundancy, the sensor node consumed more energy under idle condition, although the sensor node of the algorithm with redundancy consumed more energy when it transmitted or received packets.

From Fig.6.4 to 6.7, we could observe that the simulation time of the algorithm with redundancy was shorter than that of the algorithm without redundancy, which meant the networks lifetime of the algorithm with redundancy was shorter.

6.4.4 FLS vs Mobility

We obtained the simulation result of FLS application, which considered three antecedents. If we only considered one antecedent: the degree of mobility, the performance of average delay would be better. As plotted in Fig.6.8(a), the performance of average delay which only considered the degree of mobility was about 6% better than that of FLS application. However, the FLS application could achieve a better performance for packets received, about 18%, as plotted in Fig.6.8(b).

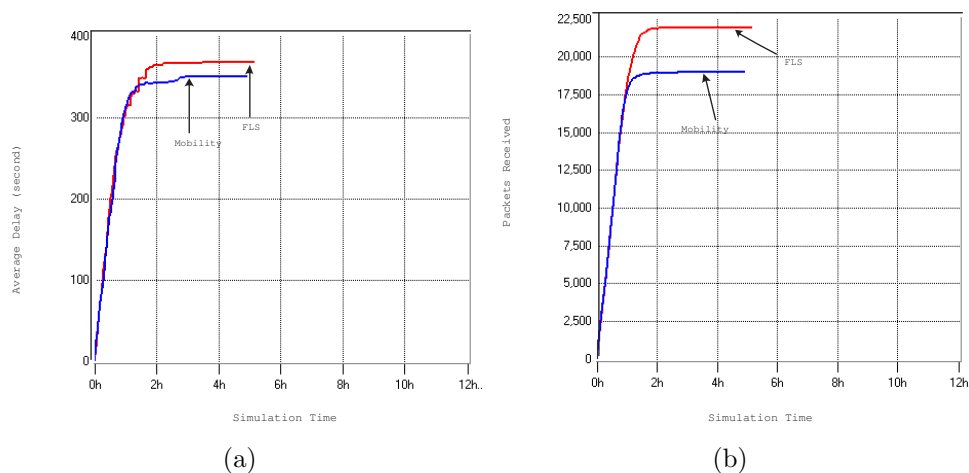


Figure 6.8. The FLS application vs the degree of mobility. (a) average delay, (b) packets received.

6.4.5 FLS vs the Remaining Energy

Similarly, we considered only one antecedent: the remaining energy, the performance of first “dead” node would be better. As plotted in Fig.6.9(a), the life time of the first “dead” node was 3 minutes longer than that of FLS application. However, the FLS application achieved a better performance for the network life, about 8 hours longer. The reason was that we adopted the path loss model in the simulation and the FLS had considered another antecedent: the distance to the source node. The nearer distance,

the less energy consumed. At the same time, the FLS application also achieved a better performance for the packets received, about 5%, as plotted in Fig.6.9(b).

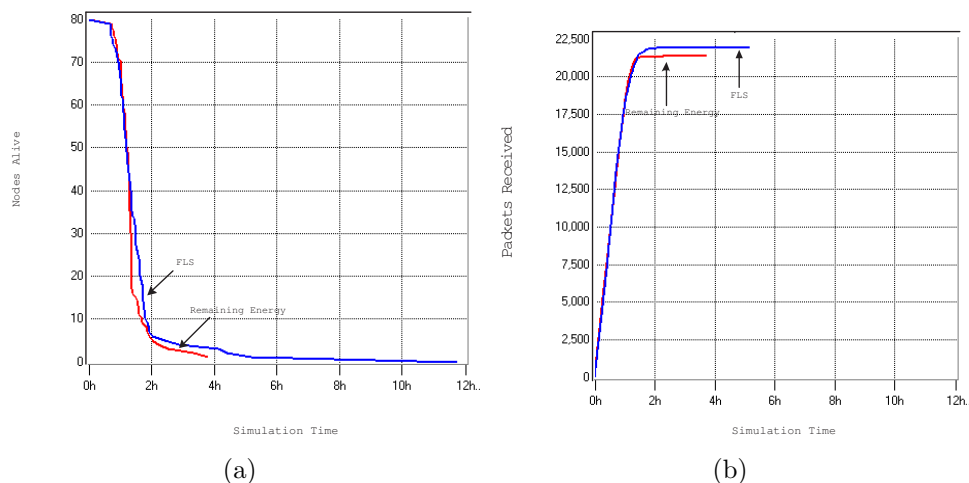


Figure 6.9. The FLS application vs the remaining energy. (a) nodes alive, (b) packets received.

Simulation results showed that the FLS application could manage the delay/energy tradeoffs to meet the networks performance requirement.

6.5 Conclusion

In order to meet different performance requirement of the service, we classified the services into high priority and low priority. Considering the effect of transmitting redundant packets, the 2-Hop relay algorithm was introduced. The algorithm with redundancy could improve the delay performance, but cost more energy to reduce the system life. In the two-hop relay algorithm, the relay/destination nodes election would determine the network performance. The simulation result showed that the two-Hop relay algorithm with/without redundancy could establish the delay/energy tradeoffs to meet different performance requirement of the services in WSN. We applied FLS to the relay/destination nodes selection. Three descriptors were used: the distance to the source

node, the remaining energy and the degree of mobility. We obtained the linguistic knowledge from a group of experts. Based on the linguistic knowledge, we set up 27 rules. The nodes possibility was the output of FLS. We elected the nodes with the highest three possibilities as the relay nodes and we elected the node with the highest possibility as the destination node. Further more, simulation results suggested that if we designed different FLS for the two-hop relay algorithm, we could meet different performance requirement in WSN.

Table 6.1. The questions for Nodes Election for the two-Hop Relay Algorithm

Antecedent 1 is *distance of a node to the source node*, Antecedent 2 is *its remaining energy*, Antecedent 3 is *its degree of mobility*, and Consequent is *the possibility that this node will be elected*. The experts were asked to fill in the blank for the Consequent using one of five linguistic labels (very weak, weak, medium, strong, very strong).

| Question # | Antecedent 1 | Antecedent 2 | Antecedent 3 | Consequent |
|------------|--------------|--------------|--------------|------------|
| 1 | near | low | high | |
| 2 | near | low | moderate | |
| 3 | near | low | low | |
| 4 | near | moderate | high | |
| 5 | near | moderate | moderate | |
| 6 | near | moderate | low | |
| 7 | near | high | high | |
| 8 | near | high | moderate | |
| 9 | near | high | low | |
| 10 | moderate | low | high | |
| 11 | moderate | low | moderate | |
| 12 | moderate | low | low | |
| 13 | moderate | moderate | high | |
| 14 | moderate | moderate | moderate | |
| 15 | moderate | moderate | low | |
| 16 | moderate | high | high | |
| 17 | moderate | high | moderate | |
| 18 | moderate | high | low | |
| 19 | far | low | high | |
| 20 | far | low | moderate | |
| 21 | far | low | low | |
| 22 | far | moderate | high | |
| 23 | far | moderate | moderate | |
| 24 | far | moderate | low | |
| 25 | far | high | high | |
| 26 | far | high | moderate | |
| 27 | far | high | low | |

Table 6.2. Histograms of expert responses about Nodes Election for the Two-Hop Relay Algorithm.

6 network experts answered the questions. The entries in the second – sixth columns correspond to the weights w_1^l , w_2^l , w_3^l , w_4^l , and w_5^l , respectively.

| Rule # (l) | very weak | weak | medium | strong | very strong | c_{avg}^l |
|----------------|-----------|------|--------|--------|-------------|-------------|
| 1 | 0 | 3 | 3 | 0 | 0 | 4.0 |
| 2 | 1 | 5 | 0 | 0 | 0 | 2.676 |
| 3 | 3 | 1 | 2 | 0 | 0 | 2.6947 |
| 4 | 0 | 0 | 3 | 3 | 0 | 6.0 |
| 5 | 0 | 0 | 0 | 5 | 1 | 7.3240 |
| 6 | 0 | 4 | 1 | 1 | 0 | 4.0 |
| 7 | 0 | 0 | 0 | 1 | 5 | 8.6199 |
| 8 | 0 | 0 | 1 | 5 | 0 | 6.6667 |
| 9 | 0 | 1 | 4 | 1 | 0 | 5.0 |
| 10 | 0 | 4 | 2 | 0 | 0 | 3.6667 |
| 11 | 3 | 2 | 1 | 0 | 0 | 2.3614 |
| 12 | 4 | 1 | 1 | 0 | 0 | 2.0374 |
| 13 | 0 | 1 | 3 | 2 | 0 | 5.3333 |
| 14 | 1 | 1 | 4 | 0 | 0 | 4.0093 |
| 15 | 2 | 3 | 0 | 1 | 0 | 3.0187 |
| 16 | 0 | 0 | 2 | 3 | 1 | 6.6573 |
| 17 | 0 | 1 | 2 | 3 | 0 | 5.6667 |
| 18 | 0 | 3 | 2 | 1 | 0 | 4.3333 |
| 19 | 2 | 4 | 0 | 0 | 0 | 2.3520 |
| 20 | 5 | 1 | 0 | 0 | 0 | 1.3801 |
| 21 | 5 | 1 | 0 | 0 | 0 | 1.3801 |
| 22 | 1 | 4 | 1 | 0 | 0 | 3.0093 |
| 23 | 1 | 4 | 1 | 0 | 0 | 3.0093 |
| 24 | 5 | 0 | 1 | 0 | 0 | 1.7134 |
| 25 | 0 | 2 | 2 | 2 | 0 | 5.0 |
| 26 | 0 | 0 | 2 | 3 | 1 | 6.6573 |
| 27 | 0 | 2 | 2 | 1 | 1 | 5.3240 |

CHAPTER 7

PACKETS TRANSMISSION IN WIRELESS SENSOR NETWORKS: INTERFERENCE, ENERGY, AND DELAY-AWARE APPROACH

Delay and energy efficiency are two important parameters to evaluate the WSNs quality. In the WSNs, the interference will affect the packets transmission. When a sensor needs to send a packet, we chose the parameter signal-to-interference ratio (SIR) as the threshold to decide whether send or not. SIR thresholds selection showed SIR could manage the tradeoff between the average delay and energy consumption. We proposed fuzzy logic system (FLS) in the optimization of SIR threshold selection. Average delay and distance of a node to the source node are selected as antecedents for the FLS. The output of FLS provided adjusting factor for the SIR threshold. Simulation results showed the fuzzy optimization could achieve a better network efficiency, reduce the average delay and extend the network lifetime [63].

7.1 Introduction

Thanks to the rapid development in low power wireless communication, microprocessor hardware in conjunction with the significant process in distributed signal process, WSNs approach to a new technological vision. While a lot of research has been concentrated on the some important aspects of WSNs, such as energy efficiency, protocol design and network deployment, the performance evaluation in WSNs is rarely studied [59]. As the WSNs is widely deployed in military and commercial application [53], energy efficiency and delay-aware become more important for WSNs.

Interference is the major limiting factor in the performance of wireless sensor networks. There are several kinds of sources of interference. In this chapter, we only consider

the interference caused by neighboring sensors. The main dilemma that the transmitter faces is when the interference is very large, the packets the destination received will be affected by the interference. So we can control the packet transmission as the following: when the transmitter observes high interference in the channel, that is the signal-to-interference ratio (SIR) is less than a threshold, it would be better to back off, buffer the traffic and wait for the interference to subside before it transmits. As it has backed off, the buffer is filling up with new packet arrivals and delay rises.

By analyzing the influence of SIR threshold selection on the network performance, we knew the SIR threshold could be a key factor. We realized the wireless model and choose three difference SIR thresholds to compare the performance. Simulation results show the SIR threshold could manage the tradeoff between the delay and energy performance.

Therefore, our primary interest lied in how to decide the SIR threshold and our goal was to optimize the value of the SIR threshold and such that energy efficiency and delay-aware could be achieved. We analyzed the performance of delay and energy according to different SIR threshold. After that, we proposed to apply fuzzy logic system (FLS) in the control of the SIR threshold. The SIR threshold would keep changing according to network performance. In this chapter, we proposed a fuzzy scheme based on the two descriptors: its average delay and distance of a node to the source node. We defined a coherent time, a certain period of time. During this coherent time, the SIR threshold was used for packet transmission. After this time, we adaptively adjusted the SIR threshold by FLS again basing on current average delay and distance of a node to the source node. By applying the fuzzy optimized mechanism to the management of the SIR threshold, a better delay and energy consumption performances were achieved.

The remainder of this chapter is structured as following. In Section 7.2, we introduced the preliminaries. In Section 7.3, we introduced the fuzzy optimization for the

energy and delay aware packets transmission. Simulation results and discussions were presented in Section 7.4. In Section 7.5, we concluded the chapter.

7.2 Preliminaries

7.2.1 Co-channel Interference

Frequency reuse implies that in a given coverage area there is several wireless sensors that use the same set of frequencies. These sensors are called co-channel sensors, and the interference between signals from these sensors is called co-channel interference [60].

For sensor i with N neighbors, if sensor i acts as the destination node during one communication, the signal to interference ratio (SIR) is represented as:

$$SIR(i) = \frac{P_r(d_{i,j})}{\sum_{k=1}^N P_r(d_{i,k})}, k \neq j \quad (7.1)$$

Where $d_{i,j}$ is the Euclidean distance between sensor i and sensor j , $P_r(d_{i,j})$ is the desired signal from sensor node j and $P_r(d_{i,k})$ is the interference power caused by the k th sensor node.

7.2.2 Queueing Model

The sensor node is keeping collecting data with a Poisson distribution, while the service is general distribution, which can be described as the M/G/1 queueing model.

Let λ be the arrival rate, μ be the service rate and the $\rho = \frac{\lambda}{\mu}$ be the traffic, if we substitute in the variance plus the squared mean for the second moment of the service time distribution [61], we can get the average queueing time:

$$W_q = \frac{L_q}{\lambda} = \frac{\lambda(\text{Var}[S_0] + \mu^{-2})}{2(1 - \rho)} \quad (7.2)$$

7.2.3 Delay

TDMA frame(Fig.7.1) has two segments: the header segment consists of request slots and the trailer segment consists of information slots. Request slots are minislots and an information slot is much longer in order to transfer data packets.

The packet transmission latency between the sensor nodes includes five parts [62]:

$$T_d = D_1 + D_2 + D_3 + D_4 + D_5 \quad (7.3)$$

D_1 : denote the time interval from the time the data packet arrives in the i th TDMA frame to the beginning of the next TDMA frame.

D_2 : denote the single TDMA frame that the data packets has to wait in the $(i+1)$ th TDMA frame.

D_3 : denote the request slot subframe that the data packet has to wait in the $(i+2)$ th TDMA frame.

D_4 : denote the time interval that the data packet has to wait for other data packets in the $(i+2)$ th frame.

D_5 : denote the time interval that the data packet has to wait for that the value of SIR is above the threshold.

In order to make the system “stable”, the rate at which sensor node transfers packets intended for its destination must satisfy all sensor that the queuing lengths will not be infinite and the average delays will be bounded [18].

7.3 Fuzzy Optimization For the Energy and Delay Aware Packets Transmission

The value of the SIR threshold will manage the energy consumption and the packet transmission delay. How to choose a proper adjusting factor for SIR threshold will determine the WSNs performance.

We collected the knowledge for adjusting factor selection based on the following two antecedents:

1. Antecedent 1. Average delay.
2. Antecedent 2. Distance of a node to the source node.

The linguistic variables used to represent the average transmission delay of a data packet was divided into three levels: *low*, *moderate*, and *high*; and those to represent distance of a node to the source node was divided into three levels: *near*, *moderate*, and *far*. The consequent – the adjusting factor for SIR threshold was divided into 5 levels, *Highly Increase*, *Increase*, *unchanged*, *Decrease*, *Highly Decrease*. Table 7.1 summarized the rules and consequents.

We designed questions such as:

IF *average delay* is *low* and *distance of a node to the source node* is *near*, THEN the adjusting factor for the SIR threshold is _____.

so we need to set up $3^2 = 9$ (because every antecedent has 3 fuzzy sub-sets, and there are 2 antecedents) rules for this FLS.

We used trapezoidal membership functions (MFs) to represent *near*, *low*, *far*, *high*, *highly increase* and *highly decrease*; and triangle MFs to represent *moderate*, *increase*, *unchanged*, and *decrease*. We show these MFs in Fig.7.2(a) and Fig.7.2(b).

In our approach to form a rule base, we chose a single consequent for each rule. We design a fuzzy logic system using rules such as:

R^l : IF *average delay* (x_1) is F_1^l , and *distance of a node to the source node* (x_2) is F_2^l ,
THEN the adjusting factor for the SIR threshold (y) is c^l .

For every input (x_1, x_2), the output is computed using

$$y_{(x_1, x_2)} = \frac{\sum_{l=1}^9 c_{G^l} \mu_{F_1^l}(x_1) \mu_{F_2^l}(x_2)}{\sum_{l=1}^9 \mu_{F_1^l}(x_1) \mu_{F_2^l}(x_2)} \quad (7.4)$$

Repeating these calculations for $\forall x_i \in [-0.1, 0.1]$, we obtained a control surface $y(x_1, x_2)$ as shown in Fig.7.3.

As showed from the control surface, the average delay for a data transmission was normalized to $[0,10]$ scale, the distance of a node to the source node was normalized to $[0,10]$ scale. The adjusting factor for the SIR threshold was characterized by the two descriptors. We applied (7.4) to compute the adjusting factor and adjust the SIR threshold. Comparing to the constant SIR threshold, the fuzzy optimization for the SIR threshold could adjust the SIR threshold dynamically to meet the delay and energy requirement.

7.4 Simulations

We implemented the simulation model using the OPNET modeler. The simulation region was 800×800 meters. There were 12 sensor nodes in the simulation model, and the sensor nodes were roaming independently with variable ground speed between 1 to 9 meters per second. The mobility model was called one-step Markov path model. The movement would change the distance between sensor and it would also change the interference power. We adopted TDMA as the multiple access techniques for wireless communications. We assumed the collecting data distribution of the mobile node was Poisson distribution and the arriving interval was 1.0 second and the length of the packet is 512 bits.

For constant SIR thresholds, we chose the SIR thresholds as three cases: high(0.5), medium(0.3) and low(0.1). Comparing the different simulation results, we concluded the influence of SIR thresholds on network performances.

After that, we chose the SIR threshold as 0.5 and applied the fuzzy optimization to adjust the SIR threshold dynamically. Comparing to the constant threshold, fuzzy optimization could improve the network performance.

7.4.1 Average Delay

Because data communications in the sensor networks have trimming constraints, it is important to design the network algorithm to meet a kind of end-end deadline [41]. We used the average delay to evaluate the network performance.

$$d_{average} = \frac{\sum_{i=1}^k d_i}{k} \quad (7.5)$$

Each packet was labeled a timestamp when the source sensor node generated it. When its destination sensor node received it, the time interval was the transmission delay.

7.4.1.1 Constant Threshold

Observing Fig.7.4(a) the delay performance of three thresholds, the lower threshold, the better delay performance. When we chose the low SIR threshold, the sensor had a high probability to send out a packet than high and medium cases. The average delay of the low threshold around 21% was shorter than that of the high case. However, the average delays of high and medium case were almost the same. The reason was that in most cases, the interference was between 0.1 and 0.3. If the service was time-sensitive, such as video or audio service, we would choose the low SIR threshold to meet their delay performance requirement.

7.4.1.2 Fuzzy Optimization

Fig.7.4(b) showed the delay performance of the constant SIR threshold and the one after fuzzy optimization. Among three thresholds, the lower threshold, the better delay performance. The Fuzzy optimization could reduce the average delay by up to 28%.

7.4.2 Energy Efficiency

It is not convenient to recharge the battery, so the energy efficiency is extremely important for sensor network. The network should keep an enough number of “live”

sensor nodes to collect data, which meant the networks needed to keep the energy among the sensor nodes in balance. We used the remaining alive sensor nodes as the parameter of the energy efficiency.

In (1.2) and (1.3), we assumed P_{elec} was equal to 6.0×10^{-4} and ϵ_{fs} was equal to 6.0×10^{-4} . We assumed that the energy of each sensor was 0.1J and the packet size was 600 bit, and the channel transmission rate was 1M bps. So when the sensor transmitted or received a packet, it would cost 6×10^{-4} second. If a sensor node transmitted N_s packets (each packet cost 6×10^{-4} second) and receives N_r packets (each packets also cost 6×10^{-4} second), we could get the remaining energy E_i of this sensor node:

$$E_i = 0.1 - (P_{tx} \times 6 \times 10^{-4} \times N_s + P_{rx} \times 6 \times 10^{-4} \times N_r) \quad (7.6)$$

When the remaining energy of a sensor node was lower than a certain threshold, the sensor was considered as “dead”. In this simulation, we chose 1.2×10^{-3} as the threshold. A sensor was “dead” meant it could not transmit/receive packets any longer, so the sensor network would ignore it. The number of sensor of wireless sensor networks which was below a certain threshold means this network does not work.

7.4.2.1 Constant Threshold

As Fig.7.5(a) showed, the remaining sensor nodes alive of the low SIR threshold was much worse that of the high case and the medium case was between the low case and high case. The reason was, the higher SIR threshold, the less energy consumed to overcome the interference. The time of the first sensor node “dead” of the high SIR threshold was over two time longer of that of the low SIR threshold case.

7.4.2.2 Fuzzy Optimization

As Fig.7.5(b) showed, after fuzzy optimization, the duration of the first node “dead” is 12% longer than that of the constant SIR threshold, which was 12000 seconds.

7.4.3 Network quality

The sensor networks were used to collect data and transfer packets. The amount of packets transmitted was one of the parameters to evaluate the networks efficiency.

7.4.3.1 Constant Threshold

Observing from Fig.7.6(a), the higher SIR threshold, the more packets collected. It was because the energy cost by each packet in the high case is less that of the low case.

7.4.3.2 Fuzzy Optimization

Observing from Fig.7.6(b), after the fuzzy optimization, the number of packets the network transmitted was 13% larger that of the constant threshold, which was 15200 packets.

We used the fuzzy logic system to adjust the SIR threshold dynamically. Compare with constant threshold, our fuzzy optimization algorithm is simpler to implement and the performance are also impressive.

7.5 Conclusion

In the WSNs, the interference will greatly affect the packets transmission. If the SIR is high, the probability of sending a packet will decrease and the packet need to be kept in the queue. The delay of the packet will increase. If the SIR is low, the delay decreases. However, in order to overcome the interference, the energy cost for each packet will increase. Simulation results of different SIR thresholds selection showed the SIR could manage the tradeoffs between the delay and energy performance. We introduced the FLS into the packets transmission. The output of the FLS was the adjusting factor for SIR threshold. Comparing with the constant threshold, fuzzy optimization could achieve a better network performance and extend network lifetime. In the future, we

could introduce noise and other interference into the wireless channel and optimize the fuzzy application.

Table 7.1. Fuzzy Rules and Consequent

| <i>Antecedent1</i> | <i>Antecedent2</i> | <i>Consequent</i> |
|--------------------|--------------------|-----------------------|
| <i>Low</i> | <i>Near</i> | <i>unchanged</i> |
| <i>Low</i> | <i>Moderate</i> | <i>Increase</i> |
| <i>Low</i> | <i>Far</i> | <i>HighlyIncrease</i> |
| <i>Moderate</i> | <i>Near</i> | <i>Decrease</i> |
| <i>Moderate</i> | <i>Moderate</i> | <i>unchanged</i> |
| <i>Moderate</i> | <i>Far</i> | <i>Increase</i> |
| <i>High</i> | <i>Near</i> | <i>HighlyDecrease</i> |
| <i>High</i> | <i>Moderate</i> | <i>Decrease</i> |
| <i>High</i> | <i>Far</i> | <i>unchanged</i> |

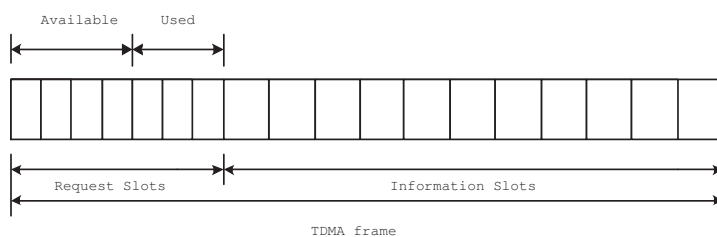
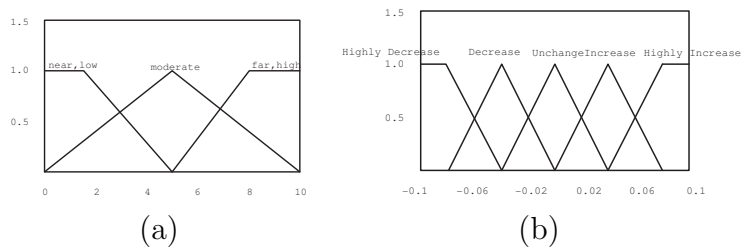


Figure 7.1. TDMA frame.



(a)

(b)

Figure 7.2. (a) MFs for Antecedents (b) MFs for Consequents.

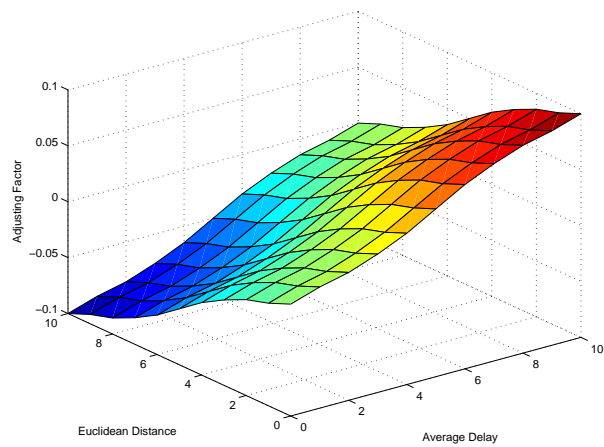
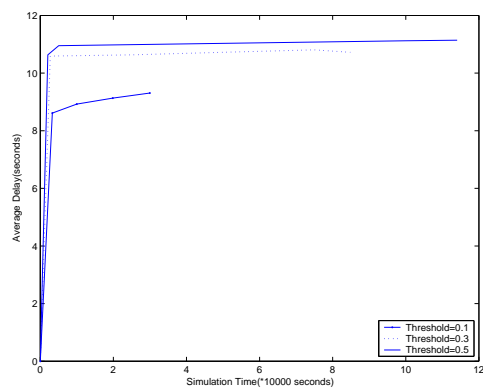
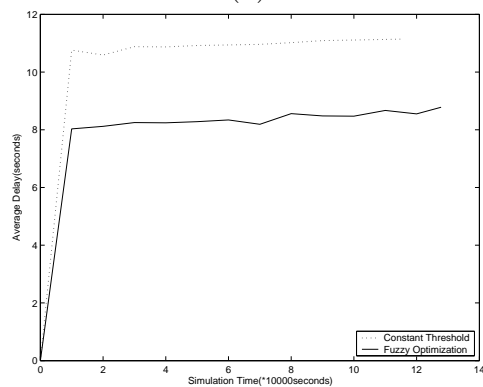


Figure 7.3. Control Surface.

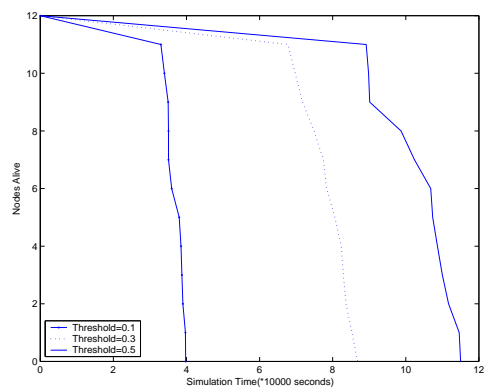


(a)

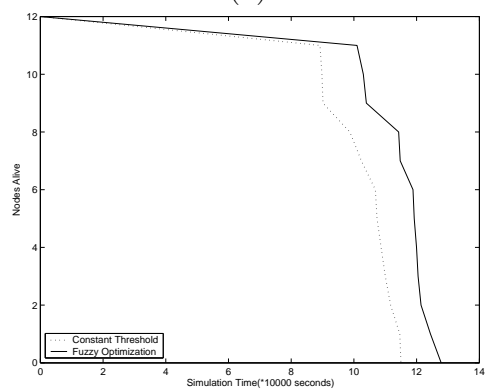


(b)

Figure 7.4. Average Delay (a) Constant Thresholds (b) Fuzzy Optimization.

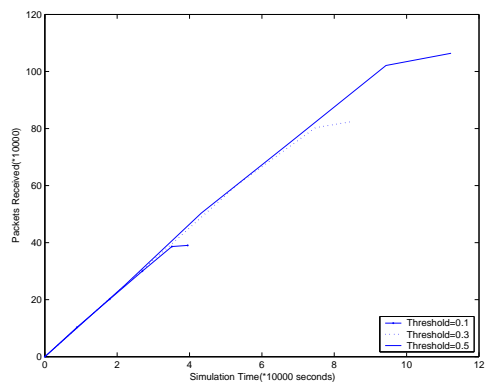


(a)

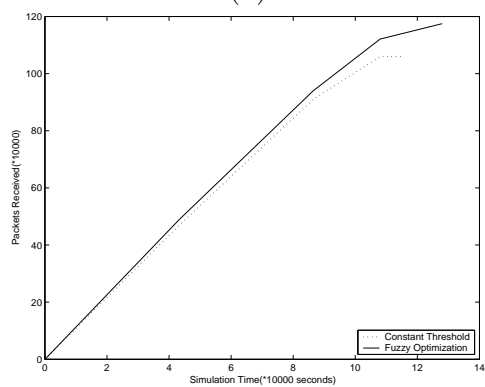


(b)

Figure 7.5. Energy Efficiency. (a) Constant Thresholds (b) Fuzzy Optimization.



(a)



(b)

Figure 7.6. Packets Received.(a) Constant Thresholds (b) Fuzzy Optimization.

CHAPTER 8

CONCLUSION AND FUTURE WORK

After nearly a decade of research efforts, WSNs have developed from an initial concept to a mature field with numerous supporting protocols. However, WSNs are still in the development due to the design complex. Cross-layer design and optimization is a new technique which can be used to design and improve the performance for WSNs. The central idea of cross-layer design is to optimize the control and exchange of information over two or more layers to achieve significant performance improvements by exploiting the interactions between various protocol layers. In this dissertation, four cross-layer design and optimization framework were proposed and the concept of using the optimization agent to provide the exchange and control of information between the protocol layers was also introduced.

8.1 Conclusions

In chapter 2, we analyzed the wireless sensor networks based on the MIMO techniques. The multiple-input and multiple-output (MIMO) system can be used to increase throughput through multiplexing or to improve PLR performance (Packet Loss Ratio) through diversity. However, MAC layer and network layer protocols will also determine the throughput and PLR. In this chapter, we coordinated physical layer, MAC layer and network layer for cross-layer evaluation.

In chapter 3, we used FLS to coordinate physical layer, data-link layer and application layer for cross-layer design. Ground speed, average delay and packets successful transmission ratio were selected as antecedents for the FLS. The output of FLS provided

adjusting factors for the AMC, transmission power, retransmission times and rate control decision.

In chapter 4, we applied a fuzzy logic system (FLS) to coordinate physical layer and data link layer. We demonstrate that type-2 fuzzy membership function (MF), i.e., the Gaussian MFs with uncertain variance is most appropriate to model BER and MAC layer service time. Two FLSs and one neural network: a singleton type-1 FLS, an interval type-2 FLS and back-prop neural network (NN) were designed to predict the packet transmission delay based on the BER and MAC layer service time.

In chapter 5, image is used as the traffic for the cross-layer design in wireless sensor networks. We combine application layer, MAC layer and physical layer together. Application level QoS was applied to evaluate the cross-layer design for WSNs.

In chapter 6, latency and energy efficiency are two QoS parameters to evaluate the Wireless Sensor Networks (WSN). Suppose the WSN has a cell-partitioned structure and the two-hop relay algorithm is adopted, the FLS was applied to the nodes selection and three descriptors are used: distance to the source node, the remaining energy and the degree of mobility. The output of FLS application provides a node election probability.

In chapter 7, we choose the parameter signal-to-interference ratio (SIR) as the threshold to decide whether send or not in WSNs. SIR thresholds selection show SIR could manage the tradeoff between the average delay and energy consumption. We proposed FLS in the optimization of SIR threshold selection. Average delay and distance of a node to the source node are selected as antecedents for the FLS.

8.2 Future Work

There is much work to be done to finally realize stable support for energy efficiency and QoS support in wireless ad hoc sensor networks. The possible work to be done is a following:

- Application layer: For Voice/Data Traffic, We could apply service differential in application layer for our cross-layer design. We set voice as high priority service, and set data as low priority service. For Video Traffic, I-frames have been proven to result in the highest number of dependencies and probability of error propagation. If the probability of degradation/loss of I-frames is decreased, it decreases the probability of degradation/loss of P-frames. We set I-frames as high priority service, and set P-frames as low priority service.
- Transport layer: User Datagram Protocol (UDP) provides a best-effort service, is used for voice traffic The Transmission Control Protocol (TCP) uses a number of protocol timers that ensure reliable and synchronized communication, which is suitable for the data traffic.
- Physical layer: MIMO techniques can improve reliability by spatial diversity and enhance throughput by spatial multiplexing. AMC technique can increase the spectral efficiency of wireless networks. Combine them together to improve the spectral efficiency at the physical layer.
- Architecture: The energy efficiency and QoS provision architecture proposed in this dissertation is a general model. The specified detail for implementing all layers, and the possible interactions are needed in WSNs. Furthermore, the implementation of all the proposed design into a hardware solution is a final goal.

APPENDIX A
AVERAGE BER PERFORMANCE

For the values of M for MQAM, one can use the approximate BER expression obtained [25]. for The AWGN, which is accurate for a wide range of SNRs, again making the substitution $\gamma \log_2 M$ for E_b/N_0 followed by averaging over the PDF of γ . Using the alternative form of the Gaussian Q-function, it is straightforward to show that the result of the evaluation is given by:

$$P_b(E) \cong 4 \left(\frac{\sqrt{M} - 1}{\sqrt{M}} \right) \left(\frac{1}{\log_2 M} \right) \sum_{i=1}^{\frac{\sqrt{M}}{2}} \frac{1}{\pi} \int_0^{\frac{\pi}{2}} M_\gamma \left(-\frac{(2i-1)^2 3E_b \log_2 M}{2 \sin^2 \theta N_0 (M-1)} \right) d\theta \quad (\text{A.1})$$

where $M_\gamma(s)$ is the MGF of the instantaneous fading power γ . For a Rayleigh fading channel, we obtain the following analogous to:

$$P_b(E) \cong 2 \left(\frac{\sqrt{M} - 1}{\sqrt{M}} \right) \left(\frac{1}{\log_2 M} \right) \sum_{i=1}^{\frac{\sqrt{M}}{2}} \left(1 - \sqrt{\frac{1.5(2i-1)^2 \frac{E_b}{N_0} \log_2 M}{M-1 + 1.5(2i-1)^2 \frac{E_b}{N_0} \log_2 M}} \right) \quad (\text{A.2})$$

Same way, one can use the approximate BER expression to get the AWGN result for MPSK:

$$P_b(E) \cong \frac{2}{\max(\log_2 M, 2)} \sum_{i=1}^{\max(\frac{M}{4}, 1)} \frac{1}{\pi} \times \int_0^{\frac{\pi}{2}} M_\gamma \left(-\frac{1}{\sin^2 \theta} \frac{E_b \log_2 M}{N_0} \sin^2 \frac{(2i-1)\pi}{M} \right) d\theta \quad (\text{A.3})$$

Specific result for the Rayleigh fading channel is:

$$P_b(E) \cong \frac{1}{\max(\log_2 M, 2)} \sum_{i=1}^{\max(\frac{M}{4}, 1)} \left(1 - \sqrt{\frac{\frac{E_b \log_2 M}{N_0} \sin^2 \frac{(2i-1)\pi}{M}}{1 + \frac{E_b \log_2 M}{N_0} \sin^2 \frac{(2i-1)\pi}{M}}} \right) \quad (\text{A.4})$$

For the value of M as 16 for 16QAM, we get:

$$P_b(E) \cong \frac{3}{8} \sum_{i=1}^2 \left(1 - \sqrt{\frac{2 \frac{E_b}{N_0} (2i-1)^2}{5 + 2 \frac{E_b}{N_0} (2i-1)^2}} \right) \quad (\text{A.5})$$

For the value of M as 64 for 64QAM, we get:

$$P_b(E) \cong \frac{5}{18} \sum_{i=1}^4 \left(1 - \sqrt{\frac{\frac{E_b}{N_0} (2i-1)^2}{7 + \frac{E_b}{N_0} (2i-1)^2}} \right) \quad (\text{A.6})$$

For BPSK and QPSK, we get the same results:

$$P_b(E) \cong \frac{1}{2} \left(1 - \sqrt{\frac{\frac{E_b}{N_0}}{1 + \frac{E_b}{N_0}}} \right) \quad (\text{A.7})$$

APPENDIX B
PUBLICATION LIST

B.1 Journal Papers

1. X. Xia, Q. Liang, "Cross-Layer Design for Mobile Ad Hoc Networks Using Interval Type-2 Fuzzy Logic Systems", Accepted by International Journal of Uncertainty, Fuzziness and Knowledge-based Systems.
2. X. Xia, Q. Liang, "Latency-aware and energy efficiency tradeoffs for sensor networks", First Round Revision for the International Journal of Sensor Networks (IJSNET).
3. X. Xia, Q. Ren, Q. Liang, "Cross-Layer Design for Mobile Ad Hoc Networks: Energy, Throughput and Delay-Aware Approach", Submitted to Journal of Applied Artificial Intelligent.
4. X. Xia, Q. Liang, "Bottom-Up Cross-Layer Optimization for Mobile Ad Hoc Networks", Submitted to Information Sciences(Elsevier).
5. X. Xia, Q. Liang, "Packets Transmission in Wireless Sensor Networks: Interference, Energy and Delay-Aware Approach", Submitted to Journal of Intelligent and Fuzzy Systems Magazine.

B.2 Conference Papers

1. X. Xia, Q. Liang, "Latency-aware and energy efficiency tradeoffs for sensor networks", Accepted by IEEE PIMRC 2004.
2. X. Xia, Q. Liang, "Latency-aware and energy efficiency evaluation for sensor networks", Accepted by IEEE 62nd VTC-2005-Fall.
3. X. Xia, Q. Ren, and Q. Liang, "Cross-Layer Design for Mobile Ad Hoc Networks: Energy, Throughput and Delay-Aware Approach", Accepted by IEEE WCNC 2006.
4. X. Xia, Q. Liang, "Bottom-Up Cross-Layer Optimization for Mobile Ad Hoc Networks", Accepted by IEEE MILCOM 2005.

5. X. Xia, Q. Liang, "Cross-Layer Design for Mobile Ad Hoc Networks Using Interval Type-2 Fuzzy Logic System", Accepted by Globecom 2006.
6. X. Xia, Q. Liang, "Packets Transmission in Wireless Sensor Networks: Interference, Energy and Delay-Aware Approach", Accepted by WCNC 2007.
7. X. Xia, Q. Liang, "Cross-Layer Evaluation for Wireless Sensor Networks based on Cooperative MIMO Techniques", Submitted to International Conference on Communications 2008.
8. X. Xia, Q. Liang, "A Fuzzy-based Latency-aware and Energy Efficiency Tradeoffs in Wireless Sensor Networks", Submitted to International Conference on Communications 2008.
9. X. Xia, Q. Liang, "Cross-Layer Design for Image Transmission in Wireless Sensor Networks", Submitted to International Conference on Communications 2008.

REFERENCES

- [1] K. Romer and F. Mattern, “The Design Space of Wireless Sensor Networks, ,” *IEEE Wireless Communications*, vol. 9, no. 4, Dec. 2004, pp. 54-61.
- [2] S. Hadim and N. Mohamed, “Middleware: middleware challenges and approaches for wireless sensor networks ,” *IEEE Distributed Systems Online*, vol 7, no. 3, Mar. 2006.
- [3] J. A. Stankovic, “Research challenges for wireless sensor networks ,” *ACM SIGBED Review* , vol. 1, no. 2, Jul. 2004, pp 9-12.
- [4] A. Cerpa and D. Estrin, “ASCENT: Adaptive Self-Configuring sEnsor Networks Topologies ,” *IEEE Transaction on Mobile Computing*, vol. 3, no. 3, Jul-Sep 2004.
- [5] K. Romer and F. Mattern “The design space of wireless sensor networks ,” *IEEE Wireless Communications*, vol 11, no. 6, Dec. 2004 pp 54-61.
- [6] A. J. Goldsmith and S. B. Wicker, “ Design Challenges for Energy-Constrained Ad Hoc Wireless Networks, ,” *IEEE Wireless Communications*, vol. 9, no. 4, 2002, pp. 8-27.
- [7] Q. Liu, S. Zhou and G. Giannakis, “ Cross-Layer Combining of Adaptive Modulation and Coding with Truncated ARQ over Wireless Links ,” *IEEE Transactions on Wireless Communications*, vol. 3, no. 5, Sept. 2004 pp. 1746 - 1755.
- [8] G. Ahn, A. Campbell, A. Veres and L. Sun, “ Support Service Differentiation for Real-Time and Best-Effort Traffic in Stateless Wireless Ad Hoc Networks (SWAN)”, *IEEE Transactions on Mobile Computing*, vol. 1 , no. 3 , July-Sept. 2002, pp. 192 - 207.

- [9] O. B. Akan and I. F. Akyildiz, “ATL, An Adaptive Transport Layer Suite for Next Generation on Wireless Internet”, *IEEE Journal on Selected Areas in Communications*, June 2004.
- [10] N. Bambos, S. Kandukuri, “Power-Controlled Multiple Access Schemes for Next-Generation Wireless Packet Networks”, *IEEE Wireless Communications*, June 2002.
- [11] J. Zhu, C. Qiao and X. Wang, “A Comprehensive Minimum Energy Routing Scheme for Wireless Ad Hoc Networks”, *IEEE INFOCOM2004*.
- [12] M. L. Sichitiu, “Cross-Layer Scheduling for Power Efficiency in Wireless Sensor Networks”, *IEEE INFOCOM2004*.
- [13] M. Scharl, and S. Shankar, “Cross-layer Wireless Multimedia Transmission: Challenges, Principles, and New Paradigms,” *Proceedings: IEEE Wireless Communications*, Aug. 2005.
- [14] D. Qiao, S. Choi, and K. G. Shin, “Goodput Analysis and Link Adaption for IEEE 802.11a Wireless LANs”, *IEEE Transactions On Mobile Computing*, Oct. 2002.
- [15] L. H. Bao, J.J. Garcia-Luna-Aceves, “Hybrid Channel Access Scheduling in Ad Hoc Networks”, *IEEE Computer Society*, Washington, DC, USA.
- [16] Chakeres, I. etc, “The Ad hoc On Demand Distance Vector (AODV) routing algorithm”, University of California at Santa Barbara , Santa Barbara , CA, USA.
- [17] W. B. Heinzelman, A. P. Chandrakasan, and H. Balakrishnan, “An application-specific protocol architecture for wireless microsensor networks ,” *IEEE Transactions on Wireless Communications*, vol. 1 no. 4, Oct 2002.
- [18] X. Xia, and Q. Liang, “Latency-aware and energy efficiency tradeoffs for sensor networks”, *Personal, Indoor and Mobile Radio Communications, 2004. PIMRC 2004*, vol. 3, pp. 1782- 1786, Spet. 2004.

- [19] X. Xia, and Q. Liang, "Latency-aware and energy efficiency evaluation for sensor networks", *IEEE 62nd Vehicular Technology Conference, 2005. VTC-2005-Fall*, vol. 3, pp. 1594- 1598, Spet. 2005.
- [20] G. L. Stuber, "*Principles of Mobile Communcation*" Kluwer Academic Press, 2001,
- [21] T. C. Hou, and T. J. Tsai, "Adaptive clustering in a hierarchical ad hoc network", *Proc. Int. Computer Symp., Tainan, Taiwan, R.O.C.*, Dec. 1998, pp. 171-176.
- [22] S. Cui, and A. J. Goldsmith, "Cross-Layer Optimization of Sensor Networks based on Cooperative MIMO Techniques with Rate Adaptation," *Proceedings: IEEE workshop on Signal Processing Advances in Wireless Communications (SPAWC)*, New York, NY, pp. 960-964, Jun 2005.
- [23] X. Xia, and Q. Liang, "Cross-Layer Evaluation for Wireless Sensor Networks based on Cooperative MIMO Techniques," *Submitted to International Conference on Communications 2008*,
- [24] S. Alamouti; "A simple Transmit Diversity Technique for Wireless Communications", *IEEE Journal on Select Area In Communication*, Vol. 16, No. 8, October 1998 .
- [25] k. Simon, et al, "*Digital Communication over Fading Channels*," Wiley Interscience, 2005.
- [26] V. Tarokh, H. Jafarkhani, and A. R. Calderbank, "Space-Time Block Coding for Wireless Communications: Performance Result", *IEEE Journal on Selected Areas in Communications*, Vol.17, No.3, March 1999.
- [27] A. Goldsmith, "Wireless Communication", *Cambridge University, 2005*.
- [28] L. Zheng, and D.N.C. Tse, " Diversity and Multiplexing: A Fundamental Tadeoff in Multiple-Antenna Channels," *IEEE Transaction On Information Theory*, Vol. 49 , No. 5 , May 2003.
- [29] G. Bianchi, "Performance Analysis of IEEE 802.11 Distributed Coordination Function", *IEEE Journal on Selected in Communications. Vol. 18, No. 3, March 2000*.

- [30] G. Zeng, and I. Chlamtac, "A Finite Queueing Model For IEEE 802.11 MAC Protocol", *IEEE 59th Vehicular Technology Conference, VTC 2004-Spring*, Vol 4, 17-19 May pp. 2037 - 2041.
- [31] H. Zhai, and Y. Fang, "Performance of Wireless LANs Based on IEEE 802.11 MAC Protocols", *14th IEEE International Symposium on Personal, Indoor and Mobile Radio Communications (PIMRC'03)*, Beijing, China, September, 2003.
- [32] D. Gross, and C. M. Harris, "Fundamental of Queueing Theory", 3rd ed., John Wiley & Sons, Inc, 1998.
- [33] I. Ari, N. Jethani, A. Rangnekar, and S. Natarajan, "Performance Analysis and Comparison of Ad-Hoc Routing Protocols," *UMBC, CMSC 691T, Mobile Computing*, Project Report.
- [34] I. Gerasimov, and R. Simon, "Performance Analysis for Ad Hoc QoS Routing Protocols," *International Mobility and Wireless Access Workshop (MobiWac'02)*, 2002.
- [35] K. Kuladinithi, and R. Gorg, "Performance Analysis of Ad hoc On-demand Distance Vector routing (AODV) using OPNET Simulator," *University of Bremen, Communication Networks*, Project Report.
- [36] X. Xia, and Q. Liang, "Bottom-Up Cross-Layer Optimization for Mobile Ad Hoc Networks", *IEEE Military Communications Conference, 2005. MILCOM 2005*, Oct. 17-20, 2005, pp. 1- 7.
- [37] X. Xia, Q. Ren, and Q. Liang, "Cross-Layer Design for Mobile Ad Hoc Networks: Energy, Throughput and Delay-Aware Approach", *Accepted by IEEE Wireless Communications and Network Conference, 2006. WCNC 2006*,
- [38] Q. Liang, "Clusterhead election for mobile ad hoc wireless network", *Personal, Indoor and Mobile Radio Communications, 2003. PIMRC 2003*, vol: 2, Sept. 7-10, 2003, pp. 1623 - 1628.

- [39] J. M. Mendel, *Uncertain Rule-Based Fuzzy Logic Systems*, Prentice-Hall, Upper Saddle River, NJ, 2001.
- [40] E. H. Mamdani, “Applications of fuzzy logic to approximate reasoning using linguistic systems”, *IEEE Trans. on Systems, Man, and Cybernetics*, vol. 26, no. 12, pp. 1182-1191, 1977.
- [41] C. Lu, et al, “RAP: a real-time communication architecture for large-scale wireless sensor networks ,” *Proceeding of the eighth IEEE real-time and embedded technology and applications Symposium*, Sep. 25 - 27, 2002, San Jose, California, pp:55 - 66.
- [42] A. Y. Wang, and C. G. Sodini, “A simple energy model for wireless microsensor transceivers,” *IEEE Global Telecommunications Conference, 2004. GLOBECOM '04*, Nov. 29 - Dec. 3, 2004, Dallas, Texas, vol 5, pp:3205 - 3209.
- [43] H. Zhai, Y. Kwon, and Y. Fang, “Performance analysis of IEEE 802.11 MAC protocols in wireless LANs,” *Wireless Communication and Mobile Computing*, pp. 917-931, 2004.
- [44] N. N. Karnik, J. M. Mendel, and Q. Liang, “Type-2 fuzzy logic systems,” *IEEE Transactions On Fuzzy Systems*, vol. 7, no. 6, pp. 643-658, Dec. 1999.
- [45] J. M. Mendel, “Fuzzy logic systems for engineering: a tutorial,” *Proc. of the IEEE*, vol. 83, no. 3, pp. 345-377, March 1995.
- [46] L. A. Zadeh, “The concept of a linguistic variable and its application to approximate reasoning - I,” *Information Sciences*, vol. 8, pp. 199-249, 1975.
- [47] Q. Liang, and J. M. Mendel, “Interval type-2 fuzzy logic systems: theory and design,” *IEEE Transactions on Fuzzy Systems*, vol. 8, no. 5, pp. 535-550, Oct 2000.
- [48] J. Jang, “ANFIS: Adaptive-Network-Based Fuzzy Inference System”, *IEEE Transactions on Systems, MAN and Cybernetics*, vol. 23, no. 3 May/June 1993.

- [49] K. Kim, and S. Kim, “Domain based approach for QoS provisioning over Mobile IP,” *Ninth IEEE International Conference on Networks, 2001*, pp. 506-510, Oct. 10-12, 2001.
- [50] V. Kawadia, and P. R. Kumar, “Principles and Protocols for Power Control in Wireless Ad Hoc Networks,” *IEEE Journal On Selected Areas in Communications*, vol. 23, no. 1, pp. 76-88, Jan 2005.
- [51] X. Xia, and Q. Liang, “ Cross-Layer Design for Image Transmission in Wireless Sensor Networks,” *Submitted to International Conference on Communications 2008*.
- [52] Z. Wang, C. Bovik et al, “ Image Quality Assessment: From Error Visibility to Structural Similarity,” *IEEE Transactions On Image Processing*, Vol. 13, No. 4. April 2004..
- [53] I. Akyildiz et al, “ A survey on sensor networks ,” *IEEE Coummun. Magazine*, pp.102-114, Aug. 2002.
- [54] M. J. Neely, and E. Modiano, “ Capacity and delay tradeoffs for Ad-Hoc mobile networks ,” *Procedding of IEEE Transactions on Information theory*.
- [55] K. Nakano, and S. Olariu, “Randomized initializtion protocols for Ad Hoc networks”, *IEEE Transactions on Parallel and distributed systems*, Vol.11, No.7, July 2000.
- [56] C. S. Raghavendra, and S. Singh, “ PAMAS-Power aware multi-access protocol with signalling for Ad-Hoc networks,” *Proceeding of the eighth IEEE real-time and embedded technology and applications Symposium*.
- [57] M. Grossglauser, and D. Tse, “ Mobility increases the capacity of Ad-hoc wireless networks ,” *IEEE/ACM Transactions on Networking*, Volume: 10 , Issue: 4 , Aug. 2002, Pages:477 - 486.

- [58] X. Xia, and Q. Liang, “ A Fuzzy-based Latency-aware and Energy Efficiency Trade-offs in Wireless Sensor Networks,” *Submitted to International Conference on Communications 2008*.
- [59] D. Chen, et al, “ QoS Support in Wireless sensor Networks: A Survey ,” *International MultiConference in Computer Science and Computer Engineering, ICWN'04*, Las Vegas, Nevada, USA, June 21-24, 2004.
- [60] T. Rappaport, “ Wireless Communications: principles and practice ,” *Second Edition*, Pearson Education, Inc., Pages: 68 - 69.
- [61] N. Prabhu, “ Basic Queueing Theory. Technical Report No. 478 ,” School of Operations Research and Industrial Engineering, Cornell University, Ithaca, New York.
- [62] T. C. Wong, et al, “ Delay performance of data traffic in a cellular wireless ATM Network ,” *Proceedings of the 3rd ACM international workshop on Wireless mobile multimedia, WOWMOM 2000*, Boston, Massachusetts, United States, pp. 101 - 107.
- [63] X. Xia, and Q. Liang, “ Packets Transmission in Wireless Sensor Networks: Interference, Energy and Delay-Aware Approach ,” *Proceedings of IEEE Wireless Communications and Networking Conference, WCNC 2007*, 11-15 March 2007 pp:2501 - 2505.

BIOGRAPHICAL STATEMENT

Xinsheng Xia received the B.E., M.E., and M.S. degrees from Huazhong University of Science and Technology, China Academy of Telecommunications Technology and The University of Toledo, OH, respectively, all in Electrical Engineering. He joined the wireless communication and networking laboratory at the University of Texas at Arlington in 2003. He is currently working toward the Ph.D degree in Electrical Engineering at UTA. His research interests include cross-layer design, fuzzy logic systems and applications, energy efficiency and QoS provision in wireless Ad Hoc and sensor networks.